Chapter 10
Models for Ebola

Another important infectious disease is Ebola virus disease (EVD). Ebola hemorrhagic fever is a very infectious disease with a case fatality rate of more than 70%. It was first identified in 1976 in the Democratic Republic of Congo and there have been more than a dozen serious outbreaks since then. The most serious outbreak to date occurred in 2014 in Guinea, Liberia, and Sierra Leone and caused more than 10,000 deaths. Response to this epidemic included the development of vaccines to combat the disease, currently being used to combat the most recent outbreak in the Democratic Republic of Congo.

A distinctive feature of the Ebola virus is much disease transmission occurs through contact with bodily fluids at funerals of Ebola victims. Many mathematical models have been used to study its disease transmission dynamics. Most of these studies have focused on estimating the basic and effective reproduction numbers of EVD, assessing the rate of growth of an epidemic outbreak, evaluating the effect of control measures on the spread of EVD, and conducting more theoretical investigations on how model assumptions may affect model outcomes (see, for example, [1, 3, 7, 8, 11, 18, 23, 25–27, 29, 31, 35, 36, 40]). Although some of these models have provided useful information and better understanding of EVD dynamics and evaluation of control programs, most of these models failed to provide reasonable projections for the 2014 outbreak in West Africa. It is important to examine the reasons for this, including the underlying assumptions made in these models. In this chapter, we describe several models for Ebola.

10.1 Estimation of Initial Growth and Reproduction Numbers

Estimation of the basic and effective reproduction numbers for EVD has been conducted for both the 2014 outbreaks in West Africa and some of the outbreaks in the past (see, for example, [1, 11, 23, 25, 36]). In [11], a standard $SEIR$ model

© Springer Science+Business Media, LLC, part of Springer Nature 2019

F. Brauer et al., *Mathematical Models in Epidemiology*, Texts in Applied Mathematics 69, https://doi.org/10.1007/978-1-4939-9828-9_10

is used for estimating $\mathscr{R}_0$ and exploring the effect of timing of the intervention on the epidemic final size. Let $S(t)$, $E(t)$, $I(t)$, and $R(t)$ denote the number of susceptible, exposed, infective, and removed individuals at time t (the dot denotes time derivatives), and let $C(t)$ denote the cumulative number of Ebola cases from the time of onset of symptoms. Assume that exposed individuals undergo an average incubation period (asymptomatic and uninfectious) of $1/k$ days before progressing to the infective class I. Infective individuals move to the R-class (death or recovered) at the per-capita rate γ. The model reads

$$\begin{aligned} S' &= -\beta S(t)I(t)/N \\ E' &= \beta S(t)I(t)/N - kE(t) \\ I' &= kE(t) - \gamma I(t) \\ R' &= \gamma I(t) \\ C' &= kE(t). \end{aligned} \tag{10.1}$$

The model (10.1) predicts initial exponential growth of the number of infectives, but in fact the initial growth rate is less than exponential. One way to modify the model to allow this is to assume behavioral changes including education of hospital personnel and community members on the use of strict barrier nursing techniques (i.e., protective clothing and equipment, patient management), and the rapid burial or cremation of patients who die from the disease. It is assumed that the net effect is a reduced transmission rate β from β_0 to $\beta_1 < \beta_0$. To take into consideration that the impact of the intervention is not instantaneous, the transmission rate is assumed to decrease gradually from β_0 to β_1 according to

$$\beta(t) = \begin{cases} \beta_0 & t < \tau \\ \beta_1 + (\beta_0 - \beta_1)e^{-q(t-\tau)} & t \geq \tau \end{cases}$$

where τ is the time at which interventions start and q controls the rate of the transition from β_0 to β_1. Another interpretation of the parameter q can be given in terms of $t_h = \frac{\log(2)}{q}$, the time to achieve $\beta(t) = \frac{\beta_0+\beta_1}{2}$.

The basic reproduction number $\mathscr{R}_0$ corresponds to β_0. If $\mathscr{R}_0$ can be estimated from data, then β_0 can be determined using the relation $\mathscr{R}_0 = \beta_0/\gamma$. For estimating $\mathscr{R}_0$, consider the E and I equations in (10.1) and the corresponding Jacobian matrix J at the disease-free equilibrium

$$J = \begin{pmatrix} -k & \beta \\ k & -\gamma \end{pmatrix}.$$

The characteristic equation is given by

$$r^2 + (k+\gamma)r + (\gamma - \beta)k = 0, \tag{10.2}$$

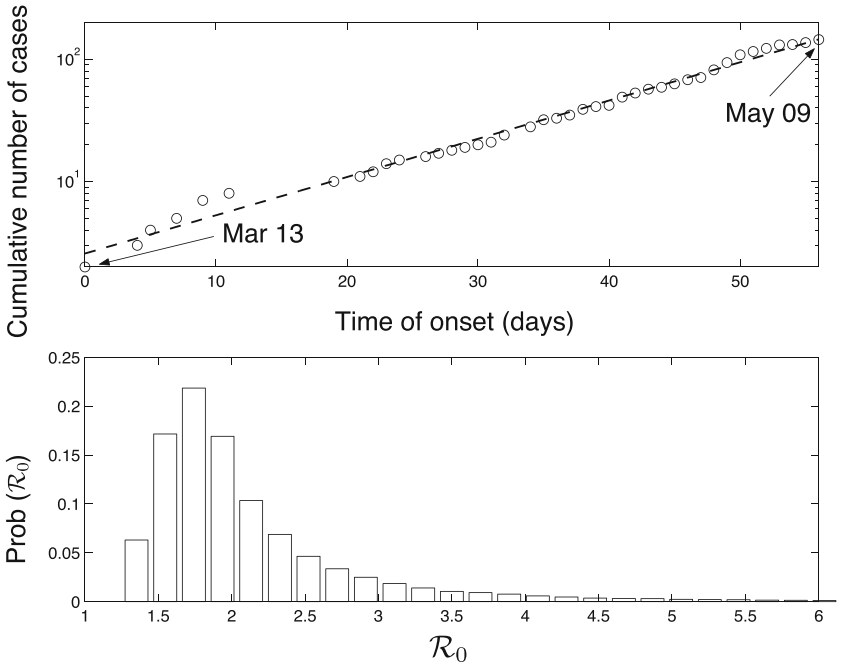

Fig. 10.1 (Top) Cumulative number of cases (log-lin scale) during the exponential growth phase of the Congo 1995 epidemic as identified by the date of start of interventions (09 May 1995 [24]). The model-free initial growth rate of the number of cases for Congo 1995 is 0.07 (linear regression); (bottom) estimated distribution of $\mathscr{R}_0$ from our uncertainty analysis (see text). $\mathscr{R}_0$ lies in the interquartile range (IQR) (1.66–2.28) with a median of 1.89. Notice that 100% of the weight lies above $\mathscr{R}_0 = 1$

and the dominant eigenvalue r represents the early-time and per-capita free growth of the outbreak. Replacing the β in (10.2) by $\gamma\mathscr{R}_0$ and solving for $\mathscr{R}_0$, we obtain

$$\mathscr{R}_0 = 1 + \frac{r^2 + (k+\gamma)r}{k\gamma}.$$

Using the time series $y(t)$ (before intervention) of the cumulative number of cases and assuming exponential growth ($y(t) \propto e^{rt}$) an estimate of r can be obtained, as shown in Fig. 10.1 (top). The estimate of the initial rate of growth r for the Congo 1995 epidemic is $r = 0.07$ day^{-1}. Based on this fixed r and Monte Carlo sampling of size 10^5 from the distributed epidemic parameters ($1/k$ and $1/\gamma$) [5], a distribution of $\mathscr{R}_0$ can be obtained as demonstrated in Fig. 10.1 (bottom), which shows that the distribution lies in the interquartile range (IQR) (1.66–2.28) with a median of 1.89.

Similar estimates for Congo 1995 data can be obtained. The estimated parameter values are listed in Table 10.1.

Table 10.1 Parameter definitions and baseline estimates obtained from the best fit of the model equations (10.1) to the epidemic-curve data of the Congo 1995 and Uganda 2000 outbreaks

		Congo 1995		Uganda 2000	
Parameter	Definition	Estim.	SD	Estim.	SD
β_0	Pre-interventions transmission rate (days^{-1})	0.33	0.06	0.38	0.24
β_1	Post-interventions transmission rate (days^{-1})	0.09	0.01	0.19	0.13
t_h	Time to achieve $\frac{\beta_0+\beta_1}{2}$ (days)	0.71	(0.02, 1.39)	0.11	(0, 0.87)
$1/k$	Mean incubation period (days)	5.30	0.23	3.35	0.49
$1/\gamma$	Mean infectious period (days)	5.61	0.19	3.50	0.67

The parameters are $0 < \beta < 1$, $0 < q < 100$, $1 < 1/k < 21$, $3.5 < 1/\gamma < 10.7$

We use the model (10.1) to evaluate intervention strategies, including surveillance and placement of suspected cases in quarantine for 3 weeks (the maximum estimated length of the incubation period). The effectiveness of interventions can be quantified in terms of the reproduction number $\mathscr{R}_p$ after interventions are implemented. For the case of Congo $\mathscr{R}_p = 0.51$ (SD 0.04) and $\mathscr{R}_p = 0.66$ (SD 0.02) for Uganda. Furthermore, the time to achieve a transmission rate of $\frac{\beta_0+\beta_1}{2}$ (t_h) is 0.71 (95% CI (0.02, 1.39)) days and 0.11 (95% CI (0, 0.87)) days for the cases of Congo and Uganda, respectively, after the time at which interventions begin.

Using the parameter values estimated from early growth, the model (10.1) can be used to simulate the Ebola outbreaks in Congo (1995) and Uganda (2000). Figure 10.2 illustrates results via Monte Carlo simulations of the stochastic model corresponding to (10.1) [33], which is constructed by considering three events: *exposure*, *infection*, and *removal*. The transition rates are defined as

Event	Effect	Transition rate
Exposure	(S, E, I, R) $\rightarrow$ (S-1, E+1, I, R)	$\beta(t)SI/N$
Infection	(S, E, I, R) $\rightarrow$ (S, E-1, I+1, R)	kE
Removal	(S, E, I, R) $\rightarrow$ (S, E, I-1, R+1)	γI

Figure 10.2 illustrates that there is very good agreement between the mean of the stochastic simulations and the reported cases. The empirical distribution of the epidemic final sizes for the cases of Congo 1995 and Uganda 2000 is given in Fig. 10.3.

The epidemic final size is sensitive to the start time of interventions τ. Numerical solutions (deterministic model) show that the epidemic final size grows exponentially fast with the initial time of interventions. For instance, for the case of Congo, the model predicts that there would have been 20 more cases if interventions had started 1 day later, as shown in Fig. 10.4.

As for most outbreaks, the initial growth of the outbreaks in Congo 1995 and Uganda 2000 is exponential. However, it is discussed that for the 2014 outbreaks in West Africa there are significant differences in the growth patterns of EVD cases at

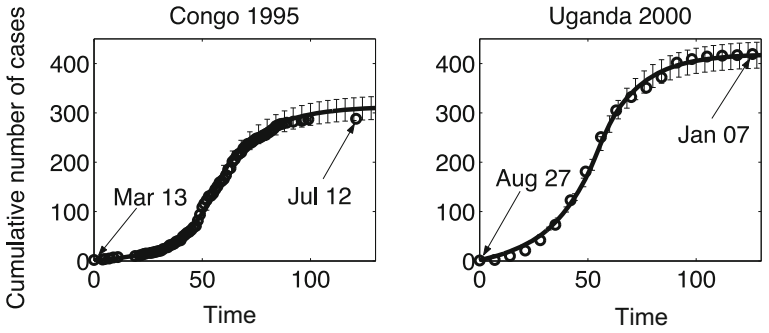

Fig. 10.2 Comparison of the cumulative number of Ebola cases during the Congo 1995 and Uganda 2000 Ebola outbreaks, as a function of the time of onset of symptoms. Circles are the data. The solid line is the average of 250 Monte Carlo replicates and the error bars represent the standard error around the mean from the simulation replicates using our parameter estimates (Table 10.1). For the case of Congo 1995, simulations were begun on 13 Mar 1995. A reduction in the transmission rate β due to the implementation of interventions occurs on 09 May 1995 (day 56) [24]. For the case of Uganda 2000, simulations start on 27 August 2000 and interventions take place on 22 October 2000 (day 56) [41]

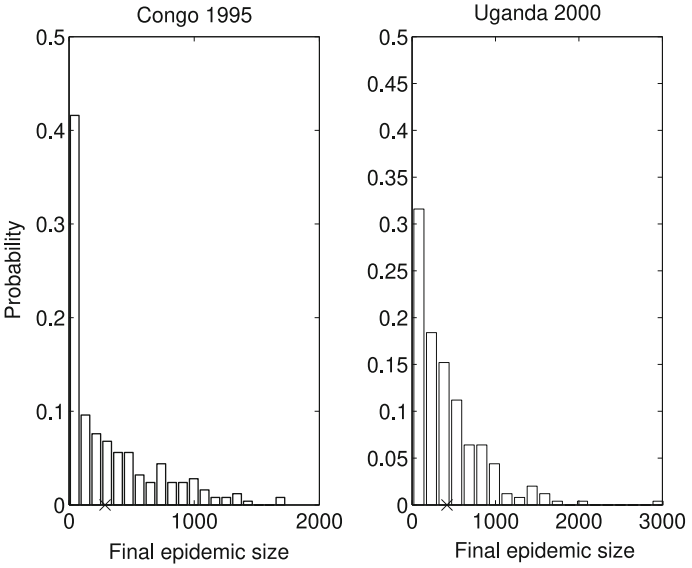

Fig. 10.3 The epidemic final size distributions for the cases of Congo 1995 and Uganda 2000 obtained from 250 Monte Carlo replicas. Crosses (X) represent the epidemic final size from data

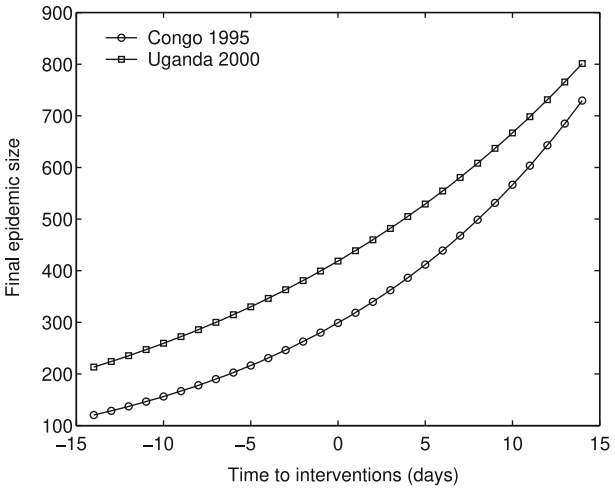

Fig. 10.4 Sensitivity of the final epidemic final size to the starting time of interventions. The negative numbers represent number of days before the actual reported intervention date and positive numbers represent a delay after the actual reported intervention date ($\tau = 0$)

the scale of the country, district, and other sub-national administrative divisions. It is illustrated that the cumulative number of EVD cases in a number of administrative areas of Guinea, Sierra Leone, and Liberia is best approximated by polynomial rather than exponential growth over several generations of EVD. It is also observed that, when data are aggregated nationally, or across the broader West Africa region, total case counts show periods of approximate exponential growth.

Temporal evolution of the effective reproduction number of Ebola is studied in [36]. In this study, a simple SEIR model with standard incidence is used in combination with the limited existing data to determine whether the transmission rate of Ebola has been changing over time in West Africa. To this end, piecewise exponential curves were fit to the time series of outbreak data to estimate the temporal evolution of the effective reproduction number of the disease. Instead of $\mathscr{R}_0$, the study focuses on assessing the time evolution of the effective reproduction number denoted by $\mathscr{R}_{eff}$, which is a dynamic estimate of the average number of secondary cases per infectious case in a population composed of both susceptible and non-susceptible individuals during the course of an outbreak. The SEIR model and its linearization about this temporary "equilibrium" are used to determine the predicted local rate of exponential rise of the epidemic curve, ρ_{eff}. For the SEIR model, this is related to $\mathscr{R}_{eff}$ by

$$\mathscr{R}_{eff} = \left(1 + \frac{\rho_{eff}}{\gamma}\right)\left(1 + \frac{\rho_{eff}}{\kappa}\right), \tag{10.3}$$

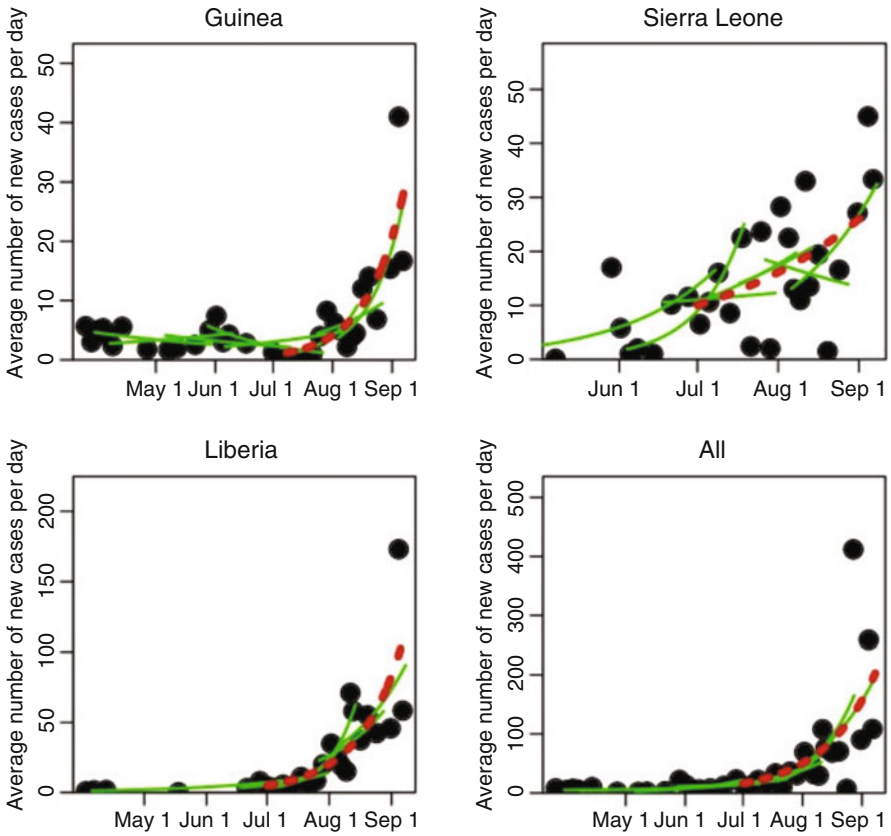

Fig. 10.5 Time series of incidence of EVD cases in West Africa

where $1/\kappa$ and $1/\gamma$ are the average incubation and infective periods of the disease, respectively. With estimates of ρ_{eff} from piecewise exponential rise fits to the incidence data from an outbreak (along with estimates of the incubation and infective periods of the disease), ρ can be estimated (Fig. 10.5), and then Eq. (10.3) can be used to obtain estimates of the temporal behavior of $\mathscr{R}_{eff}$ (Fig. 10.6), in essence approximating the temporal behavior with a piece-wise step-function.

Figure 10.5 shows time series of recorded average number of new EVD cases per day during the initial phase of the 2014 West African outbreak, for Guinea, Sierra Leone, and Liberia (dots). The green lines show a selection of the piece-wise exponential fits to the data (not all fits are shown to clarify the presentation); a moving window of groups of ten contiguous points are taken at a time, and the rate of exponential rise estimated for those ten points. The results for the estimations of the exponential rise for the full set of piece-wise fits are shown in Fig. 10.6. Shown in red is the fitted exponential rise from July 1st onwards.

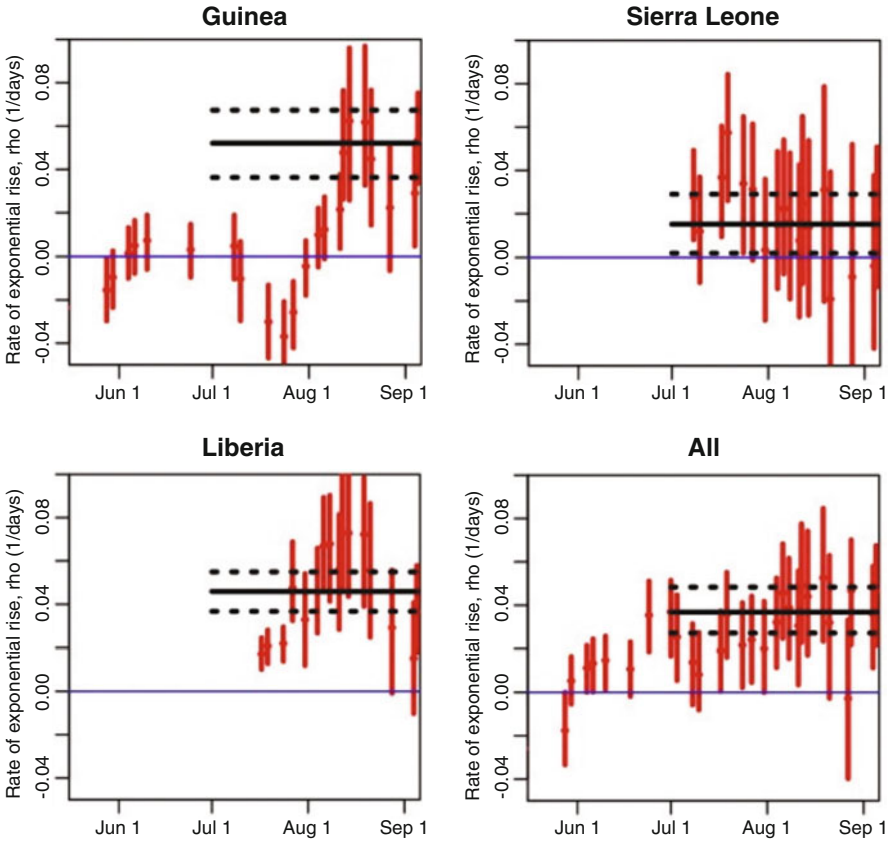

Fig. 10.6 Estimated rates of exponential rise from piece-wise exponential fits

In Fig. 10.6, estimated rates of exponential rise from piece-wise exponential fits to the average daily EVD incidence data, as shown in Fig. 10.5; a moving window of groups of ten contiguous incidence data time series points are taken at a time, and the rate of exponential rise estimated for those ten points. The dates shown on the x axis are the last date in each contiguous set of ten points, and the vertical error bars denote the 95% confidence interval. The horizontal black line shows the estimated rate of rise of an exponential fit to the incidence time series from July 1st to September 8th, with the black dotted lines indicating the 95% confidence interval.

10.1.1 Early Detection

The effect of early detection on Ebola control is studied in [10]. The model considers six epidemiological classes: susceptible individuals (S), latent undetectable individuals (E_1), latent detectable individuals (E_2), infectious symptomatic individuals (I),

isolated individuals (J), and individuals removed from isolation after recovery or disease-induced death (P), $P = R + D$, where R is the recovered class and D is the death-induced class. Susceptible individuals become infected and latent through contact with an infectious individual at the per-capita rate $(I + lJ) = N$, where β is the mean transmission rate per day, l is defined as the relative transmissibility of isolated individuals, i.e., it is a measure of the effectiveness of isolation of infective individuals, and N is the total population size. Latent undetectable individuals (E_1) enter the latent detectable class E_2 at a rate k_1, and become infectious symptomatic at a rate k_2. A fraction of the latent detectable individuals are diagnosed (i.e., by RT-PCR), $p_T = f_T = (f_T + k_2)$, and become isolated. We assume that the latent detectable class represents individuals with a viral load above the detection limit of the specific diagnostic test. Infective individuals are isolated at a rate α, or they are removed after recovery or disease-induced death at a rate γ. Similarly, individuals are removed from isolation after recovery or disease-induced death, but at a rate γ_r. The model reads

$$\begin{aligned}
S' &= -\beta S\frac{I + lJ}{N} \\
E_1' &= \beta S\frac{I + lJ}{N} - k_1 E_1 \\
E_2' &= k_1 E_1 - k_2 E_2 - f_T E_2 \\
I' &= k_2 E_2 - (\alpha + \gamma) I \\
J' &= \alpha I + f_T E_2 - \gamma_r J \\
R' &= \gamma(1 - \delta) I + \gamma_r (1 - \delta) J \\
D' &= \gamma \delta I + \gamma_r \delta J \\
N &= S + E_1 + E_2 + I + J + R.
\end{aligned} \tag{10.4}$$

The analysis suggests that the impact of early diagnosis of pre-symptomatic infections is strongly dependent on the effectiveness of isolation of infective individuals in health-care settings. For instance, with an isolation effectiveness of 50% and with an average time of 3 days from the onset of symptoms to isolation, the attack rate (total number of Ebola cases/population size) remains essentially unchanged as the rate of pre-symptomatic case detection increases (Fig. 10.7). In contrast, early detection of pre-symptomatic individuals can have a significant impact on the transmission dynamics of Ebola if the effectiveness of isolating infective cases is at least 60%. Even at this level of isolation, at least 50% of pre-symptomatic cases would need to be detected in the community, a scenario difficult to achieve with limited resources. When the effectiveness of isolation is increased to 65%, detecting about 25% of pre-symptomatic cases is predicted to lead to epidemic control, i.e., the effective reproduction number is reduced below the epidemic threshold.

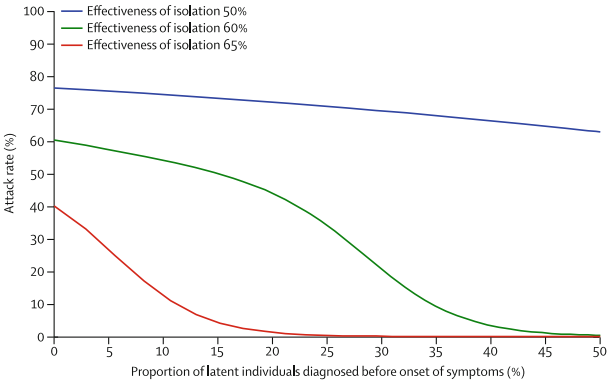

Fig. 10.7 Predictions of the effect of diagnosing pre-symptomatic individuals on the attack rate of the Ebola epidemic. The mean time from onset of symptoms to isolation was set at 3 days

10.2 Evaluations of Control Measures

One of the typical characteristics for EVD is that significant transmissions can occur by infectious individuals after death but before burial. Also, no effective drugs or vaccine were available for the outbreak in West Africa. The main control measures include isolation, hospitalization, contact tracing, and safe burial. Several mathematical models have been used to assess the effectiveness of these control measures (e.g., [3, 7, 26, 27, 35, 40]). Most of the models in these studies use SEIR type of models with various modifications. One of the EVD models on which many other models are based is the one considered in Legrand et al. [26], which will be discussed in more detail in the next section.

A model considered in [7] has the following form (with modified notation):

$$\begin{aligned} S' &= -\beta S(I_h + I_u)/N \\ E' &= \beta S(I_h + I_u)/N - \alpha E \\ I_h' &= p\alpha E - \delta_h I_h \\ I_u' &= (1-\rho)\alpha E - \delta_u I_u \\ H' &= \delta_h I_h, \end{aligned} \tag{10.5}$$

where N is the total population size and is assumed to be constant. In this model, two separate compartments for infective individuals are considered, namely infective individuals which will be hospitalized/reported (I_h) and infectious individuals which will not be hospitalized and unreported (I_u). The H compartment represents the cumulative hospitalized/reported cases (so it includes those who are recovered after being hospitalized). The model (10.5) also assumes that individuals in both I_h and I_u have the same transmission rate β, p is the fraction of hospitalized cases, $1/\delta_h$ is time from infectiousness (symptom) onset until hospitalization/isolation

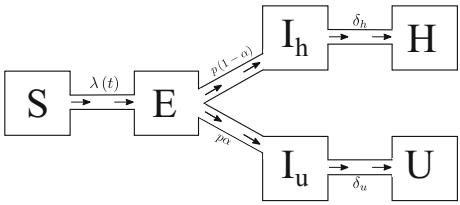

Fig. 10.8 A transition diagram for model (10.5)

and reporting, and $1/\delta_u$ is the mean infective period for an unhospitalized case. A transition diagram of the model is depicted in Fig. 10.8.

For model (10.5), the reproduction number is given by

$$\mathscr{R}_e = \mathscr{R}_0\left(p\frac{\delta_u}{\delta_h} + 1 - p\right),$$

where $\mathscr{R}_0 = \beta/\delta_u$ is the basic reproduction number. An extension of the model (10.5) is also considered in [7] to take into consideration contact tracing.

The following deterministic model is considered in [25].

$$\begin{aligned} S' &= -\mathscr{R}_0\delta SI/N, \\ E_1' &= \mathscr{R}_0\delta SI/N - m\alpha E_1, \\ E_i' &= m\alpha(E_{i-1} - E_i), \quad i = 2, \cdots, m \\ I' &= m\alpha E_m - \delta I, \\ R' &= \delta I. \end{aligned} \tag{10.6}$$

In model (10.6), the stage distribution of the latent stage is assumed to be gamma with the shape parameter equal to m, which leads to a division of the exposed class E into m sub-classes with mean duration $1/(m\alpha)$. By examining the model fit to the weekly case reports in Guinea, Liberia, and Sierra Leone from the WHO situation report dated from 1 October 2014 (http://www.who.int/csr/disease/ebola/situation-reports/en/), the authors pointed out that fitting of such deterministic models to cumulative incidence data can lead to bias and pronounced underestimation of the uncertainty associated with model parameters.

The models (10.5) and (10.6) ignored the special characteristic associated with the fact that significant transmissions can occur by those who are dead but not yet buried. This is considered in the Legrand model, which is discussed in detail next.

10.3 The Legrand Model and Underlying Assumptions

Many mathematical models have been used for the recent epidemics of Ebola in West Africa. However, the success of these models in the case of the 2014 Ebola outbreak in West Africa was very limited. As pointed out in [8], "mathematical models have failed to accurately project the outbreak's course." Although various reasons may explain why "on-the-ground data contradict the projections of published models," including incomplete and unreliable data on Ebola epidemiology (especially in the hardest-hit areas) and lack of empirical data on how disease-control measures quantitatively affect Ebola transmission, it is important to examine the appropriateness of assumptions made in the models on which the projections are based. This is the objective of this section. There have been various modeling approaches, including deterministic and stochastic models, or relatively simple models consisting of ordinary differential equations (ODEs) and more complicated agent-based models, among others. Many of the ODE models are variations of the model studied by the Legrand model (10.7). It has been pointed out that some of the assumptions made in the Legrand model may not have clear justifications (e.g., [35]). Thus, it is important to examine the critical assumptions made in this model and better understand their possible impact on model outcomes.

10.3.1 The Legrand Model

The Legrand et al. model [26] consists of a system of ordinary differential equations with six compartments representing the epidemiological classes of susceptible (S), exposed (E), infective (I), hospitalized (H), dead but not yet buried (D), and removed (R). The transition diagram of the model is depicted in Fig. 10.9.

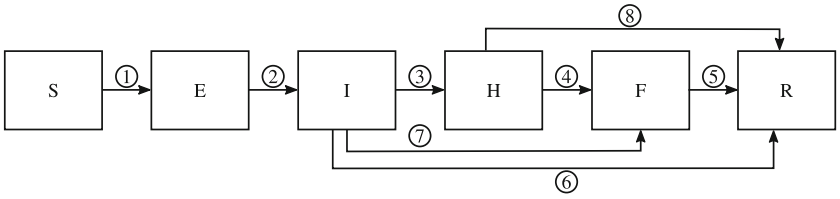

Fig. 10.9 A transition diagram for the model in Legrand et al. [26]

The model presented by Legrand et al. [26] reads

$$\begin{aligned}
\frac{dS}{dt} &= -\frac{1}{N}S(\beta_I I + \beta_H H + \beta_D D) \\
\frac{dE}{dt} &= \frac{1}{N}S(\beta_I I + \beta_H H + \beta_D D) - \alpha E \\
\frac{dI}{dt} &= \alpha E - (\gamma_h\theta_1 + \gamma_i(1-\theta_1)(1-\delta_1) + \gamma_d(1-\theta_1)\delta_1)I \\
\frac{dH}{dt} &= \gamma_h\theta_1 I - (\gamma_{dh}\delta_2 + \gamma_{ih}(1-\delta_2))H \\
\frac{dD}{dt} &= \gamma_d(1-\theta_1)\delta_1 I + \gamma_{dh}\delta_2 H - \gamma_f D \\
\frac{dR}{dt} &= \gamma_i(1-\theta_1)(1-\delta_1)I + \gamma_{ih}(1-\delta_2)H + \gamma_f D.
\end{aligned} \tag{10.7}$$

The parameters β_I, β_H, and β_D denote the transmission rates in the I, H, and D classes, respectively; let $1/\alpha$ be the mean latent period; and let $1/\gamma_f$ be the mean time between death and burial.

The three key parameters that are in the Legrand model (10.7), θ_1, δ_1, and δ_2, do not have direct biological meaning but are computed based on the probabilities of hospitalization and of disease-induced mortality with or without hospitalization. For example, the fraction of infective people hospitalized is

$$p = \frac{\gamma_h\theta_1}{\gamma_h\theta_1 + \gamma_i(1-\theta_1)(1-\delta_1) + \gamma_d(1-\theta_1)\delta_1}, \tag{10.8}$$

and the probabilities of death with (f_h) and without hospitalization (f_i) are given by

$$\begin{aligned}
f_h &= \frac{\gamma_{dh}\delta_2}{\gamma_{dh}\delta_2 + \gamma_{ih}(1-\delta_2)} \\
f_i &= \frac{\gamma_d\delta_1}{\gamma_i(1-\delta_1) + \gamma_d\delta_1}.
\end{aligned} \tag{10.9}$$

If we assume $f_i = f_h = f$, then θ_1, δ_1, and δ_2 can be determined in terms of p and f using (10.8) and (10.9).

In addition, the Legrand model imposes the following constraints:

$$\frac{1}{\gamma_i} = \frac{1}{\gamma_h} + \frac{1}{\gamma_{ih}} \quad \text{and} \quad \frac{1}{\gamma_d} = \frac{1}{\gamma_h} + \frac{1}{\gamma_{dh}}, \tag{10.10}$$

and assumes that hospitalization does not affect the time from onset to recovery or from onset to death. Other assumptions made in model (10.7) are associated with exponential waiting times. It is assumed that, after entering the infective class I, individuals can leave due either to hospitalization (entering H) or recovery without being hospitalized (entering R from I) or death without being hospitalized (entering D from I) with average waiting times $1/\gamma_h$, $1/\gamma_i$, $1/\gamma_d$, respectively. Or equivalently, after onset, individuals enter the H, R, and D classes at constant rates γ_h, γ_i, and γ_d, respectively. Their model assumes that the overall rate of leaving the I class, denoted by Δ, is a weighted average of the three rates γ_h, γ_i, and γ_d as

$$\Delta = \theta_1\gamma_h + (1-\theta_1)\delta_1\gamma_d + (1-\theta_1)(1-\delta_1)\gamma_i, \tag{10.11}$$

where θ_1 is the proportion of cases hospitalized, and δ_1 is a coefficient that is determined such that

$$\frac{\delta_1\gamma_d}{\delta_1\gamma_d + (1-\delta_1)\gamma_i}$$

is equal to case fatality (i.e., the proportion of cases that die).

10.3.2 A Simpler System Equivalent to the Legrand Model

It is shown in [18] that the Legrand model (10.7) is equivalent to the following model:

$$\begin{aligned}
\frac{dS}{dt} &= -\frac{1}{N}S(\beta_I I + \beta_H H + \beta_D D),\\
\frac{dE}{dt} &= \frac{1}{N}S(\beta_I I + \beta_H H + \beta_D D) - \alpha E,\\
\frac{dI}{dt} &= \alpha E - \gamma I,\\
\frac{dH}{dt} &= p\gamma I - \omega H,\\
\frac{dD}{dt} &= (1-p)f\gamma I + f\omega H - \gamma_f D,\\
\frac{dR}{dt} &= (1-p)(1-f)\gamma I + (1-f)\omega H,
\end{aligned} \tag{10.12}$$

where

$$\begin{aligned}
\frac{1}{\gamma} &= p\frac{1}{\gamma_{IH}} + (1-p)f\frac{1}{\gamma_{ID}} + (1-p)(1-f)\frac{1}{\gamma_{IR}},\\
\frac{1}{\omega} &= f\frac{1}{\omega_{HD}} + (1-f)\frac{1}{\omega_{HR}}.
\end{aligned} \tag{10.13}$$

Using the following connections between parameters in (10.12) and the Legrand model (10.7):

$$\gamma_{IR} = \gamma_i, \quad \gamma_{IH} = \gamma_h, \quad \gamma_{ID} = \gamma_d,$$

the conditions in (10.13) can be written as

$$\begin{aligned} \frac{1}{\gamma} &= p\frac{1}{\gamma_h} + (1-p)f_i\frac{1}{\gamma_d} + (1-p)(1-f_i)\frac{1}{\gamma_i}, \\ \frac{1}{\omega} &= f_h\frac{1}{\gamma_{dh}} + (1-f_h)\frac{1}{\gamma_{ih}}, \end{aligned} \tag{10.14}$$

and the constraints (10.10) becomes

$$\frac{1}{\gamma_{IR}} = \frac{1}{\gamma_{IH}} + \frac{1}{\omega_{HR}}, \quad \frac{1}{\gamma_{ID}} = \frac{1}{\gamma_{IH}} + \frac{1}{\omega_{HD}}. \tag{10.15}$$

The only minor difference between the two models is where to move the buried (whether or not to R), which does not affect the dynamic behavior of the model.

10.4 *Models with Various Assumptions on Stage Transition Times

In the Legrand model (10.7) or the equivalent model (10.12), it is not clear what underlying assumptions have been made regarding the distributions of waiting times for epidemiological processes including the time from onset to recovery (transition from I to R), to hospitalization (transition from I to H), and to death (transition from I to D). For ease of reference, we refer to these three transitions as IR, IH, and ID, respectively. In addition, the two possible transitions for hospitalized individuals, recovery or death, are denoted by HR and HD. In this section, we derive three integro-differential equations models under different assumption on those transition times and compare the difference in the model outcomes.

Let T_P, T_L, and T_M denote random variables for the waiting times associated with IR, IH, and ID, and let the associated survival functions be denoted by $P(t)$, $L(t)$, and $M(t)$, respectively. The mean duration of these transitions are, respectively, $\mathbb{E}[T_P]$, $\mathbb{E}[T_L]$, and $\mathbb{E}[T_D]$. Similarly, let $\mathscr{D}_{HR}$ and $\mathscr{D}_{HD}$ denote the mean duration from hospitalization to recovery or death, respectively. For ease of comparison between models presented in this paper, we list in Table 10.2 some of the quantities that play common roles and have clear biological meaning in these models. Several of these quantities should have values that are independent of model assumptions, including the mean duration (absent intervention) from onset to recovery $\mathbb{E}[T_P]$, the probability of hospitalization p, and the probability of death f.

Table 10.2 Definition of symbols commonly used in the models in this section

Symbol	Definition
T_P, T_L, T_M	Random variables for the waiting times in I before moving to R, H, D, respectively
X_I	Random variable for the overall time spent in the I compartment
X_H	Random variable for the overall time spent in the H compartment
$P_i(s)$	Probability that a living individual remains infectious s units of time since onset for models I, II, III when $i = 1, 2, 3$, respectively. That is, $\mathbb{P}\big[T_{P_i} > s\big] = P_i(s)$
$L_i(s)$	Probability of a living individual not being hospitalized s units of time since onset for models I, II when $i = 1, 2$, respectively. That is, $\mathbb{P}\big[T_{L_i} > s\big] = L_i(s)$
$M_1(s)$	Probability of surviving the disease s units of time since onset for model I. That is, $\mathbb{P}\big[T_{M_1} > s\big] = M_1(s)$
$Q_3(s)$	Probability of not having recovered s time units after being hospitalized for model III
$\mathbb{E}[T_P]$	Mean duration from onset to recovery (absent intervention or death)
$\mathbb{E}[T_L]$	Mean duration from onset to hospitalization (given hospitalized and not dead)
$\mathbb{E}[T_M]$	Mean duration between onset and death (absent intervention or recovery)
$\mathbb{E}[X_I]$	Mean duration in the I compartment (hospitalization and death included)
$\mathbb{E}[X_H]$	Mean duration in the H compartment (death included)
$\mathscr{D}_{HR}$	Mean duration from hospitalization to recovery
$\mathscr{D}_{HD}$	Mean duration from hospitalization to death
γ_{IR}	$= 1/\mathbb{E}[T_P]$
γ_{IH}	$= 1/\mathbb{E}[T_L]$
γ_{ID}	$= 1/\mathbb{E}[T_M]$
ω_{HR}	$= 1/\mathscr{D}_{HR}$, per-capita rate of transition from H to R if the transition is exponential
ω_{HD}	$= 1/\mathscr{D}_{HD}$, per-capita rate of transition from H to D if the transition is exponential
p	Proportion hospitalized (dependent on control effort)
f	Probability of death (with or without hospitalization)
γ	$= 1/\mathbb{E}[X_I]$, per-capita rate of exiting I if X_I is exponential

If the transitions IR, IH, and ID are assumed to be independent in the Legrand model and the waiting times are all exponentially distributed with mean durations $1/\gamma_{IR}$, $1/\gamma_{IH}$, and $1/\gamma_{ID}$, respectively, then the mean overall time spent in the I compartment is

$$\mathbb{E}\big[\min\{T_P, T_L, T_M\}\big] = \int_0^\infty P(t)L(t)M(t)dt = \frac{1}{\gamma_{IR} + \gamma_{IH} + \gamma_{ID}}.$$

Thus, the overall rate of exiting I is $\gamma_{IR} + \gamma_{IH} + \gamma_{ID}$, which is not a weighted average given by Δ in (10.11) for the Legrand model. This implies that the Legrand model has made different assumptions on these transitions.

In the formulation of the integro-differential equations models, we will adopt probabilistic terminology to facilitate the interpretation of these models, and focus on the following three scenarios:

(I) Assume that the three transitions IR, IH, and ID are *independent* and the waiting times are described by the survival functions $P_1(s)$, $L_1(s)$, and $M_1(s)$, respectively, where s represents the time-since-onset. It is also assumed that hospitalization does not affect the time from onset to recovery or death.

(II) The two transitions IR and ID are *combined* and described by a single survival function $P_2(s)$, with a fraction $1 - f$ of the exiting individuals recovering (and the fraction f dying). The transition IH is independent of IR and ID and the waiting time is described by the survival function $L_2(s)$. Similar to model I, it is also assumed that hospitalization does not affect the time from onset to recovery or probability of death.

(III) All three transitions (IH, IR, and ID) are combined and described by a single survival function $P_3(s)$, with a fraction p of the exiting individuals being hospitalized and a fraction $1 - f$ (respectively, f) of the non-hospitalized individuals recovering (respectively, dying). The two transitions HR and HD are combined and the waiting time is described by a single survival function $Q_3(s)$ with a fraction $1 - f$ (or f) of the exiting individuals recovering (or dying). P_3 and Q_3 are assumed to be independent. Unlike models I and II, in which the time from onset to hospitalization is tracked due to the independent stage distributions, in model III a constraint must be imposed so that the time between onset and hospitalization plus the time between hospitalization and recovery (or death) equals the time between onset and recovery (or death).

To focus on the general waiting time for the infective stage and its influence on model formulation when hospitalization is considered, assume simpler distributions for other stages including the latent stage and the duration between death and burial. That is, the E and D stages are assumed to have exponential distributions with constant rates α and γ_f. As the models are derived under arbitrary distributions for the waiting times of key disease stages, they consist of systems of integro-differential equations. It shows that these systems reduce to ODE systems when the arbitrary stage distributions are replaced by gamma or exponential distributions. Detailed derivations of the systems of integral equations are provided in Feng et al. (2016).

The model I, which corresponds to the scenario (I) described above, assumes independent IR, IH, and ID processes. Let T_{P_1}, T_{L_1}, and T_{M_1} denote random variables for the independent waiting times of IR, IH, and ID, respectively, that are described by the following survival functions:

- $P_1(s)$: Probability that a living individual remains infectious s units of time since onset (governing both IR and HR).
- $L_1(s)$: Probability of a living individual not being hospitalized s units of time since onset (governing the IH transition).
- $M_1(s)$: Probability of surviving the disease s units of time since onset (governing both ID and HD).

Figure 10.10 depicts the transitions between epidemiological classes for the model under scenario (I). All variables and parameters have the same meanings as before unless otherwise stated. The diagram in (a) depicts transitions between compartments when stage durations for the IR, IH, and ID transitions are arbitrarily described by the survival functions $P_1(t)$, $L_1(t)$, and $M_1(t)$. The dotted rectangle around the I and H compartments indicates that individuals in these two compartments are being tracked for their time-since-onset using the same survival

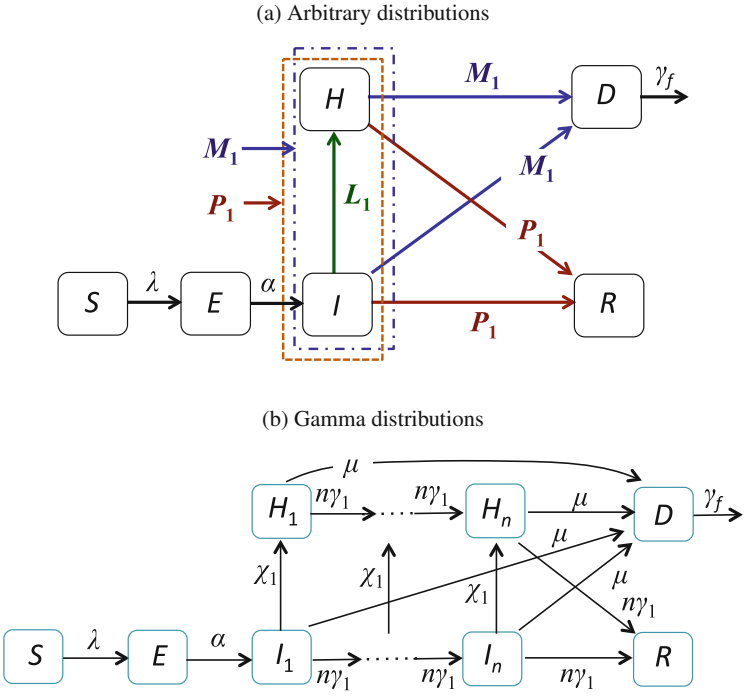

Fig. 10.10 Transition diagram for Model I when T_{P_1}, T_{L_1}, and T_{M_1} are arbitrary (**a**), or gamma/exponential (**b**). The corresponding survival functions are $P_1(t)$ (red), $L_1(t)$ (green), and $M_1(t)$, respectively

function $P_1(t)$, i.e., the time elapsed in I before entering H is taken into account when determining the time between entering H and recovery. The diagram in (b) illustrates the effect of the "linear chain trick" when $P_1(t)$ follows a gamma distribution, and $L_1(t)$ and $M_1(t)$ follow exponential survival functions.

The model with the general stage distributions P_1, L_1, and M_1 consists of the following system of integro-differential equations:

$$\frac{dS}{dt} = -\lambda(t)S, \qquad \frac{dE}{dt} = \lambda(t)S - \alpha E,$$

$$I(t) = \int_0^t \alpha E(s)P_1(t-s)L_1(t-s)M_1(t-s)ds + I(0)P_1(t)L_1(t)M_1(t),$$

$$\begin{aligned} H(t) = &\int_0^t \alpha E(s)P_1(t-s)M_1(t-s)\big[1 - L_1(t-s)\big]ds \\ &+ I(0)P_1(t)M_1(t)\big[1 - L_1(t)\big], \end{aligned} \tag{10.16}$$

$$D(t) = \int_0^t \left[\int_0^\tau \alpha E(s)P_1(\tau - s)g_{M_1}(\tau - s)ds + I(0)P_1(\tau)g_{M_1}(\tau)\right] e^{-\gamma_f(t-\tau)}d\tau,$$

$$R(t) = \int_0^t \left[\int_0^\tau \alpha E(s)g_{P_1}(\tau - s)M_1(\tau - s)ds + I(0)g_{P_1}(\tau)M_1(\tau)\right] d\tau,$$

where $\lambda(t)$ is given by

$$\lambda(t) = \frac{\beta_I I + \beta_H H + \beta_D D}{N}, \tag{10.17}$$

The initial condition is $(S(0), E(0), I(0), H(0), D(0), R(0)) = (S_0, E_0, I_0, 0, 0, 0)$, where S_0 and E_0 are positive constants. Notice that in system (10.16), the probability distributions for T_{P_1}, T_{L_1}, and T_{M_1} are arbitrary.

Consider the case when T_{P_1} follows a gamma distribution with shape and rate parameters $(n, n\gamma_1)$ (where $n \geq 1$ is an integer), and T_{L_1} and T_{M_1} follow exponential distributions with parameters χ_1 and μ, respectively (which are gamma distributions with shape parameter 1). That is,

$$\begin{aligned} P_1(t) &= G^n_{n\gamma_1}(t) = \sum_{j=1}^{n} \frac{(n\gamma_1 t)^{j-1} e^{-n\gamma_1 t}}{(j-1)!}, \\ L_1(t) &= G^1_{\chi_1}(t) = e^{-\chi_1 t}, \\ M_1(t) &= G^1_{\mu}(t) = e^{-\mu t}. \end{aligned} \tag{10.18}$$

Then, it is shown in [18] that (10.16) is equivalent to the following system of ODEs:

$$\begin{aligned}
\frac{dS}{dt} &= -\frac{1}{N}S\Big(\beta_I \sum_{j=1}^{n} I_j + \beta_H \sum_{j=1}^{n} H_j + \beta_D D\Big),\\
\frac{dE}{dt} &= \frac{1}{N}S\Big(\beta_I \sum_{j=1}^{n} I_j + \beta_H \sum_{j=1}^{n} H_j + \beta_D D\Big) - \alpha E,\\
\frac{dI_1}{dt} &= \alpha E - (n\gamma_1 + \chi_1 + \mu)I_1,\\
\frac{dI_j}{dt} &= n\gamma_1 I_{j-1} - (n\gamma_1 + \chi_1 + \mu)I_j, \quad \text{for } j = 2, \ldots n,\\
\frac{dH_1}{dt} &= \chi_1 I_1 - (n\gamma_1 + \mu)H_1,\\
\frac{dH_j}{dt} &= \chi_1 I_j + n\gamma_1 H_{j-1} - (n\gamma_1 + \mu)H_j, \quad \text{for } j = 2, \ldots n,\\
\frac{dD}{dt} &= \mu \sum_{j=1}^{n} I_j + \mu \sum_{j=1}^{n} H_j - \gamma_f D,\\
\frac{dR}{dt} &= n\gamma_1 I_n + n\gamma_1 H_n.
\end{aligned} \tag{10.19}$$

In the special case when $n = 1$ (i.e., P_1 is also an exponential distribution), the model (10.19) simplifies to

$$\begin{aligned}
\frac{dS}{dt} &= -\frac{1}{N}S(\beta_I I + \beta_H H + \beta_D D),\\
\frac{dE}{dt} &= \frac{1}{N}S(\beta_I I + \beta_H H + \beta_D D) - \alpha E,\\
\frac{dI}{dt} &= \alpha E - (\gamma_1 + \chi_1 + \mu)I,\\
\frac{dH}{dt} &= \chi_1 I - (\gamma_1 + \mu)H,\\
\frac{dD}{dt} &= \mu I + \mu H - \gamma_f D,\\
\frac{dR}{dt} &= \gamma_1 I + \gamma_1 H.
\end{aligned} \tag{10.20}$$

Note that in model (10.20) the per-capita transition rates from I to R and from H to R are both equal to γ_1, from which we have $\gamma_{IR} = \omega_{HR}$. This means that the constraints in (10.15) for model (10.12) cannot be satisfied. Thus, model I cannot be equivalent to the Legrand model. This suggests that Legrand et al. did *not* assume that the three transitions of IR, IH, and ID were described by independent exponential distributions and that the overall waiting time in the I compartment was the minimum of these three exponential waiting times.

When P_1, L_1, and M_1 are exponential with the respective parameters γ_1, χ_1, and μ, because of the assumption in model I that the three transitions IR, IH, and ID are independent, the overall waiting time in the I compartment is also exponential with the rate constant $\gamma_1 + \chi_1 + \mu$. From the definition of these parameters, we can link them to the general parameters (i.e., independent of model assumptions) in Table 10.2. There might be multiple ways of making the connections. One example is the following: For example,

$$\frac{1}{\gamma_1} = \frac{1}{\gamma_{IR}} = \mathbb{E}[T_{P_1}], \quad f = \frac{\mu}{\gamma_1 + \mu}, \quad p = \frac{\chi_1}{\gamma_1 + \chi_1 + \mu}, \tag{10.21}$$

where γ_{IR}, f, and p are parameters that are independent of models. From the relations in (10.21) we can express the rates γ_1, χ_1, and μ in terms of only γ_{IR}, p, and f:

$$\gamma_1 = \gamma_{IR}, \quad \chi_1 = \gamma_{IR}\frac{p}{(1-f)(1-p)}, \quad \mu = \gamma_{IR}\frac{f}{1-f}. \tag{10.22}$$

Reproduction Numbers for Models (10.16), (10.19), and (10.20)

Based on the biological meaning of $\mathscr{R}_C$, we obtain the following expression for $\mathscr{R}_{C1}^{\text{general}}$ for model (10.16) under general stage distributions:

$$\begin{aligned}\mathscr{R}_{C1}^{\text{general}} &= \beta_I \mathbb{E}\left(\min\left\{T_{P_1}, T_{L_1}, T_{M_1}\right\}\right) \\ &\quad + \beta_H\left[\mathbb{E}\left(\min\left\{T_{P_1}, T_{M_1}\right\}\right) - \mathbb{E}\left(\min\left\{T_{P_1}, T_{L_1}, T_{M_1}\right\}\right)\right] + \beta_D \tfrac{1}{\gamma_f} p_M,\end{aligned} \tag{10.23}$$

where

$$\mathbb{E}\left(\min\left\{T_{P_1}, T_{L_1}, T_{M_1}\right\}\right) = \int_0^\infty P_1(t)L_1(t)M_1(t)dt$$

represents the average time spent in the I compartment, and

$$\mathbb{E}\left(\min\left\{T_{P_1}, T_{M_1}\right\}\right) = \int_0^\infty P_1(t)M_1(t)dt$$

represents the average total time spent in the I and H compartments.

For the model (10.19) with gamma distribution,

$$\begin{aligned}\mathscr{R}_{C1}^{\text{Gamma}} &= \frac{\beta_I}{\chi_1+\mu}\left[1-\left(\frac{n\gamma_1}{n\gamma_1+\chi_1+\mu}\right)^n\right] \\ &+\frac{\beta_H}{\mu}\left[\frac{\chi_1}{\chi_1+\mu}+\frac{\mu}{\chi_1+\mu}\left(\frac{n\gamma_1}{n\gamma_1+\chi_1+\mu}\right)^n-\left(\frac{n\gamma_1}{n\gamma_1+\mu}\right)^n\right] \\ &+\frac{\beta_D}{\gamma_f}\left[1-\left(\frac{n\gamma_1}{n\gamma_1+\mu}\right)^n\right].\end{aligned} \tag{10.24}$$

For the model (10.20) with exponential distribution,

$$\begin{aligned}\mathscr{R}_{C1}^{\text{Exp}} &= \frac{\beta_I}{\gamma_1+\chi_1+\mu}+\frac{\beta_H}{\gamma_1+\mu}\frac{\chi_1}{\gamma_1+\chi_1+\mu}+\frac{\beta_D}{\gamma_f}\frac{\mu}{\gamma_1+\mu} \\ &= \frac{\beta_I}{\gamma_1+\chi_1+\mu}+\frac{\beta_H p}{\gamma_1+\mu}+\frac{\beta_D f}{\gamma_f}.\end{aligned} \tag{10.25}$$

Next, consider different assumptions on the transition processes. In model I, the three transitions IR, IH, and ID are assumed to be independent, in which case the three transitions "compete" for individuals in the I class. Another scenario is to consider only two independent transitions, one being hospitalization and the other combining recovery and death for those who are not hospitalized. In this case, we have two survival probability functions:

- $P_2(s)$: Probability of still being infectious *and* alive s time units after onset (governing all four transitions IR, ID, HR, and HD).
- $L_2(s)$: Probability of not being hospitalized s time units after onset (governing the IH transition).

Assume that, for those who exit I without being hospitalized, a fixed fraction $1-f$ (or f) will recover (or die) an assumption of Legrand model. Assume also that individuals in I and H classes have the same probability of death (f), also as assumed in the Legrand model. The transition diagram is depicted in Fig. 10.11a.

(a) Arbitrary distributions

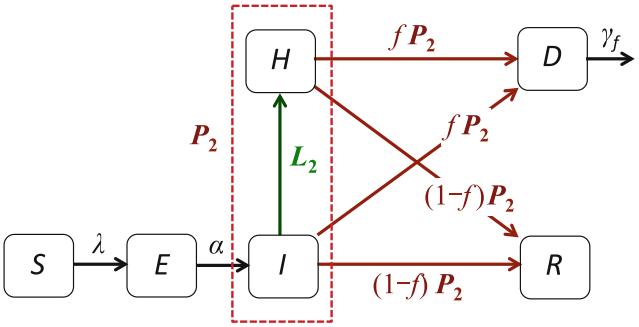

(b) Gamma distributions

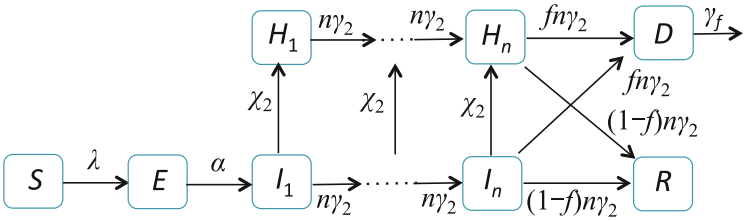

Fig. 10.11 A transition diagram for model II when T_{P_2} and T_{L_2} are arbitrary distributions (**a**) and when they are gamma or exponential (**b**). In (**a**), the recovery/death (red) and hospitalization (green) transitions are governed by the survival functions P_2 and L_2. In (**b**), the recovery/death (red) and hospitalization (green) transitions are indicated by the same colors as in (**a**)

Model II has the form

$$\begin{aligned}
\frac{dS(t)}{dt} &= -\lambda(t)S(t),\\
\frac{dE(t)}{dt} &= \lambda(t)S(t) - \alpha E(t),\\
I(t) &= \int_0^t \alpha E(s)P_2(t-s)L_2(t-s)ds + I(0)P_2(t)L_2(t),\\
H(t) &= \int_0^t \alpha E(s)P_2(t-s)\big[1-L_2(t-s)\big] + I(0)P_2(t)\big[1-L_2(t)\big],\\
D(t) &= f\int_0^t \left[\int_0^\tau \alpha E(s)g_{P_2}(\tau-s)ds + I(0)g_{P_2}(\tau)\right] e^{-\gamma_f(t-\tau)}d\tau,\\
R(t) &= (1-f)\int_0^t \left[\int_0^\tau \alpha E(s)g_{P_2}(\tau-s)ds + I(0)g_{P_2}(\tau)\right] d\tau.
\end{aligned} \tag{10.26}$$

The function $\lambda(t)$ is the same as in model I and given in (10.17). We can reduce the integral equations in (10.26) to the ODEs given below:

$$\begin{aligned}
\frac{dS}{dt} &= -\frac{1}{N}S\Big(\beta_I \sum_{j=1}^{n} I_j + \beta_H \sum_{j=1}^{n} H_j + \beta_D D\Big),\\
\frac{dE}{dt} &= \frac{1}{N}S\Big(\beta_I \sum_{j=1}^{n} I_j + \beta_H \sum_{j=1}^{n} H_j + \beta_D D\Big) - \alpha E,\\
\frac{dI_1}{dt} &= \alpha E - (n\gamma_2 + \chi_2)I_1,\\
\frac{dI_j}{dt} &= n\gamma_2 I_{j-1}(t) - (n\gamma_2 + \chi_2)I_j, \quad \text{for } j = 2, \ldots n,\\
\frac{dH_1}{dt} &= \chi_2 I_1 - n\gamma_2 H_1,\\
\frac{dH_j}{dt} &= \chi_2 I_j + n\gamma_2 H_{j-1} - n\gamma_2 H_j, \quad \text{for } j = 2, \ldots n,\\
\frac{dD}{dt} &= fn\gamma_2 I_n + fn\gamma_2 H_n - \gamma_f D,\\
\frac{dR}{dt} &= (1-f)n\gamma_2 I_n + (1-f)n\gamma_2 H_n.
\end{aligned} \tag{10.27}$$

The reproduction numbers $\mathscr{R}_{C2}$ for model II also have different forms than those for model I. In the case of general distributions,

$$\begin{aligned}
\mathscr{R}_{C2}^{\text{general}} &= \beta_I \mathbb{E}\left(\min\left\{T_{P_2}, T_{L_2}\right\}\right) + \beta_H \left[\mathbb{E}\left(T_{P_2}\right) - \mathbb{E}\left(\min\left\{T_{P_2}, T_{L_2}\right\}\right)\right]\\
&\quad + \beta_D \tfrac{1}{\gamma_f}\left[f(1-p_{H2}) + f p_{H2}\right].
\end{aligned} \tag{10.28}$$

When P_2 is a gamma distribution,

$$\begin{aligned}
\mathscr{R}_{C2}^{\text{Gamma}} &= \beta_I \frac{1}{\chi_2}\left[1 - \left(\frac{n\gamma_2}{n\gamma_2 + \chi_2}\right)^n\right]\\
&\quad + \beta_H \left[\frac{1}{\gamma_2} - \frac{1}{\chi_2}\left[1 - \left(\frac{n\gamma_2}{n\gamma_2 + \chi_2}\right)^n\right]\right] + \beta_D \frac{f}{\gamma_f}.
\end{aligned} \tag{10.29}$$

When P_2 is exponential, the model (10.27) becomes

$$\begin{aligned}
\frac{dS}{dt} &= -\frac{1}{N}S(\beta_I I + \beta_H H + \beta_D D),\\
\frac{dE}{dt} &= \frac{1}{N}S(\beta_I I + \beta_H H + \beta_D D) - \alpha E,\\
\frac{dI}{dt} &= \alpha E - (\gamma_2 + \chi_2)I,\\
\frac{dH}{dt} &= \chi_2 I - \gamma_2 H,\\
\frac{dD}{dt} &= f\gamma_2 I + f\gamma_2 H(t) - \gamma_f D(t),\\
\frac{dR}{dt} &= (1-f)\gamma_2 I + (1-f)\gamma_2 H.
\end{aligned} \tag{10.30}$$

The formula for $\mathscr{R}_{C2}$ in (10.28) simplifies to

$$\mathscr{R}_{C2}^{\text{Exp}} = \frac{\beta_I}{\gamma_2 + \chi_2} + \frac{p\beta_H}{\gamma_2} + \frac{f\beta_D}{\gamma_f}. \tag{10.31}$$

As in model I, there can be multiple choices for linking the parameter γ_2 to the common parameters. For example,

$$\frac{1}{\gamma_2} = (1-f)\frac{1}{\gamma_{IR}} + f\frac{1}{\gamma_{ID}},$$

where $1/\gamma_{ID}$ denotes the average time from onset to death. Also, $p = \chi_2/(\gamma_2+\chi_2)$. Thus,

$$\gamma_2 = \frac{1}{(1-f)/\gamma_{IR} + f/\gamma_{ID}}, \quad \chi_2 = \frac{\gamma_2 p}{1-p}. \tag{10.32}$$

Another set of possible assumptions that are different from models I and II is to consider two independent distributions for the waiting times in I and H compartments, denoted by T_{P_3} and T_{Q_3}, with survival functions

- $P_3(s)$: Probability of remaining in the I class s units of time since onset (governing the transitions IR, IH, and ID).
- $Q_3(s)$: Probability remaining in the H class s units of time after being hospitalized (governing the HR and HD transitions).

Let $p_3(t) = -P_3'(t)$ and $q_3(t) = -Q_3'(t)$ denote the probability density functions. P_3 describes the waiting time for the combined transitions, IR, IH, and ID. Assume that among the individuals exiting the I class, fractions of p, $(1-p)f$, $(1-p)(1-f)$ will be hospitalized, non-hospitalized and dead, and non-hospitalized and recovered, respectively ($0 \le p, f < 1$). Q_3 describes the waiting time for the combined two

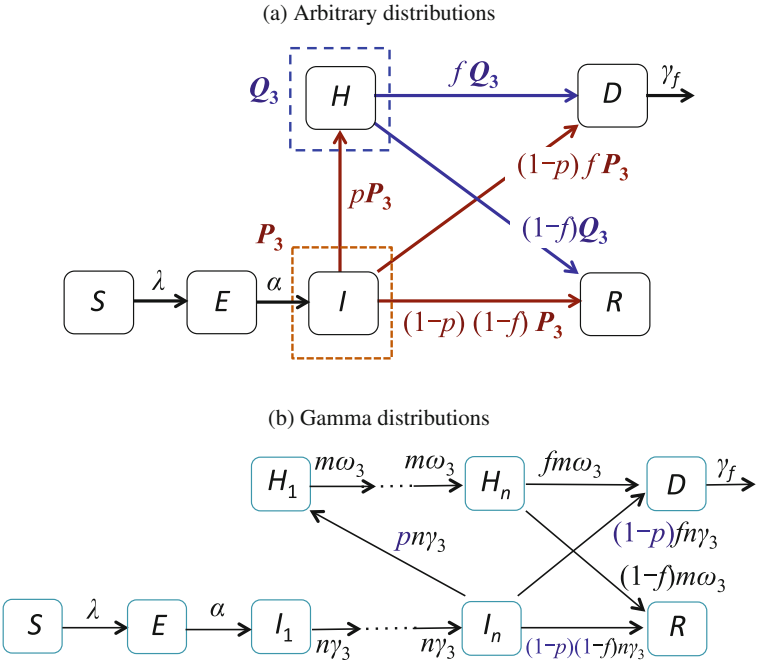

Fig. 10.12 A transition diagram for model III when T_{P_3} and T_{Q_3} are arbitrary distributions (**a**) and when they are gamma or exponential (**b**)

transitions, HR and HD, and we assume that fractions $1-f$ and f of the hospitalized individuals recover or die, respectively. A transition diagram is shown in Fig. 10.12.

In this case, model III consists of the following system of integro-differential equations:

$$
\begin{aligned}
&S'(t) = -\lambda(t)S(t), \qquad E'(t) = \lambda(t)S(t) - \alpha E(t),\\
&I(t) = \int_0^t \alpha E(s)P_3(t-s)ds + I(0)P_3(t),\\
&H(t) = \int_0^t p\left[\int_0^s \alpha E(\tau)p_3(s-\tau)d\tau + I(0)p_3(s)\right]Q_3(t-s)ds\\
&D'(t) = (1-p)f\left[\int_0^t \alpha E(s)p_3(t-s)ds + I(0)p_3(t)\right]\\
&\quad + f\int_0^t \left[p\int_0^s \alpha E(\tau)p_3(s-\tau)d\tau + pI(0)p_3(s)\right]q_3(t-s)ds - \gamma_f D(t),\\
&R'(t) = (1-p)(1-f)\left[\int_0^t \alpha E(s)p_3(t-s))ds + I(0)p_3(t)\right]\\
&\quad + (1-f)\int_0^t \left[p\int_0^s \alpha E(\tau)p_3(s-\tau)d\tau + pI(0)p_3(s)\right]q_3(t-s)ds.
\end{aligned}
\tag{10.33}
$$

Note that it is easier in this case to write equations for D' and H' than for D and H.

Assume that T_{P_3} and T_{Q_3} follow gamma distributions with shape parameters n and m respectively, i.e., the survival functions are given by

$$\begin{aligned} P_3(t) &= G^n_{n\gamma_3}(t) = \sum_{j=1}^{n} \frac{[n\gamma_3(t-s)]^{j-1} e^{-n\gamma_3(t-s)}}{(j-1)!}, \\ Q_3(t) &= G^m_{m\omega_3}(t) = \sum_{j=1}^{m} \frac{[m\omega_3(t-s)]^{j-1} e^{-m\omega_3(t-s)}}{(j-1)!}. \end{aligned} \tag{10.34}$$

Then, the system (10.33) reduces to the following system of ODEs:

$$\begin{aligned} \frac{dS}{dt} &= -\frac{1}{N} S\Big(\beta_I \sum_{j=1}^{n} I_j + \beta_H \sum_{j=1}^{m} H_j + \beta_D D\Big), \\ \frac{dE}{dt} &= \frac{1}{N} S\Big(\beta_I \sum_{j=1}^{n} I_j + \beta_H \sum_{j=1}^{m} H_j + \beta_D D\Big) - \alpha E, \\ \frac{dI_1}{dt} &= \alpha E - n\gamma_3 I_1, \\ \frac{dI_k}{dt} &= n\gamma_3 I_{k-1} - n\gamma_3 I_k, \quad k = 2, \ldots, n \\ \frac{dH_1}{dt} &= pn\gamma_3 I_n - m\omega_3 H_1, \\ \frac{dH_k}{dt} &= m\omega_3 H_{k-1} - m\omega_3 H_k, \quad k = 2, \ldots, m \\ \frac{dD}{dt} &= (1-p) f n\gamma_3 I_n + f m\omega_3 H_n - \gamma_f D, \\ \frac{dR}{dt} &= (1-p)(1-f) n\gamma_3 I_n + (1-f) m\omega_3 H_m. \end{aligned} \tag{10.35}$$

A transition diagram under the gamma distributions for T_{P_3} and T_{Q_3}, for the ODE model (10.35) is shown in Fig. 10.12b. We observe a major difference between this figure and Fig. 10.10b or Fig. 10.11b in the recovery rates from I_n and H_m, which have different values here. A similar difference exists in the transition rates from I_j to I_{j+1} ($j = 1, \cdots, n-1$) and from H_j to H_{j+1} ($j = 1, \cdots, m-1$).

In the special case when $n = m = 1$ (i.e., P_3 and Q_3 are exponential), the ODE model (10.35) simplifies to

$$\begin{aligned}
\frac{dS}{dt} &= -\frac{1}{N}S(\beta_I I + \beta_H H + \beta_D D),\\
\frac{dE}{dt} &= \frac{1}{N}S(\beta_I I + \beta_H H + \beta_D D) - \alpha E,\\
\frac{dI}{dt} &= \alpha E - \gamma_3 I,\\
\frac{dH}{dt} &= p\gamma_3 I - \omega_3 H,\\
\frac{dD}{dt} &= (1-p)f\gamma_3 I + f\omega_3 H - \gamma_f D,\\
\frac{dR}{dt} &= (1-p)(1-f)\gamma_3 I + (1-f)\omega_3 H.
\end{aligned} \tag{10.36}$$

Notice that, if we ignore the last term in the R equation in the equivalent Legrand model (10.12) (this term indicates that the R class includes those buried), the model (10.36) is identical to the model (10.12) when the subscript "3" is dropped; that is, when γ_3 and ω_3 *are defined* as follows:

$$\begin{aligned}
\frac{1}{\gamma_3} &= \frac{p}{\gamma_{IH}} + \frac{(1-p)f}{\gamma_{ID}} + \frac{(1-p)(1-f)}{\gamma_{IR}},\\
\frac{1}{\omega_3} &= \frac{f}{\omega_{HD}} + \frac{1-f}{\omega_{HR}},
\end{aligned} \tag{10.37}$$

together with the constraints

$$\frac{1}{\gamma_{IR}} = \frac{1}{\gamma_{IH}} + \frac{1}{\omega_{HR}}, \quad \frac{1}{\gamma_{ID}} = \frac{1}{\gamma_{IH}} + \frac{1}{\omega_{HD}}. \tag{10.38}$$

The reproduction number $\mathscr{R}_{C3}$ for model III can be derived using the same approach as for models I and II. Because the derivations are similar, we omit the details, and present the formula only for the special case when P_3 and Q_3 are both exponential, i.e., $P_3 = G^1_{\gamma_3}$ and $Q_3 = G^1_{\omega_3}$ (see (10.34)). In this case, the formula for $\mathscr{R}_{C3}$ for the ODE model (10.35) is *independent* of m and n, and is given by

$$\mathscr{R}^{\text{Exp}}_{C3} = \frac{\beta_I}{\gamma_3} + p\frac{\beta_H}{\omega_3} + f\frac{\beta_D}{\gamma_f}, \tag{10.39}$$

where γ_3 and ω_3 are given in (10.37).

Note that the main difference between models I, II, and III lies in the assumptions on the underlying biological processes, particularly the sojourn distributions for

various stage transitions, which are described by functions $L(t)$, $P(t)$, $M(t)$, and $Q(t)$. The fact that the Legrand model can only be obtained from model III, not from models I and II, identifies the specific assumptions made in the Legrand model in terms of these sojourn distributions. For example, our analyses suggest the following assumptions made in the Legrand model:

(a) The overall sojourn in the I stage is assumed to be exponentially distributed with the average duration $1/\gamma$, which is further assumed to be the specific weighted average of $1/\gamma_{IR}$, $1/\gamma_{IH}$, and $1/\gamma_{ID}$ as given in (10.13), where $1/\gamma_{IR}$, $1/\gamma_{IH}$, and $1/\gamma_{ID}$ are the respective average stage duration of the IR, IH, and ID transitions. However, from model I we see that if the IR, IH, and ID transitions follow independent exponential distributions with parameters γ_{IR}, γ_{IH}, and γ_{ID}, then the overall sojourn in the I stage is exponentially distributed with the parameter $\gamma = \gamma_{IR} + \gamma_{IH} + \gamma_{ID}$ with the average duration

$$\frac{1}{\gamma} = \frac{1}{\gamma_{IR} + \gamma_{IH} + \gamma_{ID}},$$

which differs from (10.13).

(b) The distributions for the I and H stages are independent (see $P_3(t)$ and $Q_3(t)$). This implies that the average time spent in the H stage before recovery or death $(1/\omega_3)$ does not depend on the average time spent in the I stage before recovery or being hospitalized or dying $(1/\gamma_3)$. Under this assumption, the time spent in H before recovery $(1/\gamma_{HR})$ does not take into consideration the time spent in I before being hospitalized $(1/\gamma_{IH})$. Because of this independence, the model needs to impose a constraint to link these two durations (see (10.10)).

Difference in Evaluations by Models I, II, and III

Among the three ODE models (10.20), (10.30), and (10.36), which are reduced from the models I, II, and III with general distributions, the only model that can match the Legrand model is (10.36), for which the assumptions include: (i) the waiting times of the three transitions IR, IH, and ID are *not* independent and (ii) the overall waiting time in the I compartment is a weighted average of the mean durations $(1/\gamma_{IR}, 1/\gamma_{IH}$, and $1/\gamma_{ID})$ for the three transitions with weights determined by the probabilities of hospitalization p and death f, as described in (10.14). By examining the ODE model (10.20), we found that, if the waiting times of the three transitions IR, IH, and ID are independent and exponentially distributed (with parameters γ_1, χ_1, and μ), then the overall waiting time in I should be an exponential distribution with the parameter $\gamma_1 + \chi_1 + \mu$. That is, the average overall waiting time should be $1/(\gamma_1 + \chi_1 + \mu)$, *not* a weighted average such as the ones in (10.14).

Formulas for the control reproduction numbers $\mathscr{R}_{Ci}$ $(i = 1, 2, 3)$ for the three general models provide a means of examining the influence of assumptions on model outcomes. For example, consider the three control reproduction numbers $\mathscr{R}_{Ci}$ $(i = 1, 2, 3)$, which are given in (10.25), (10.31), and (10.39) corresponding to

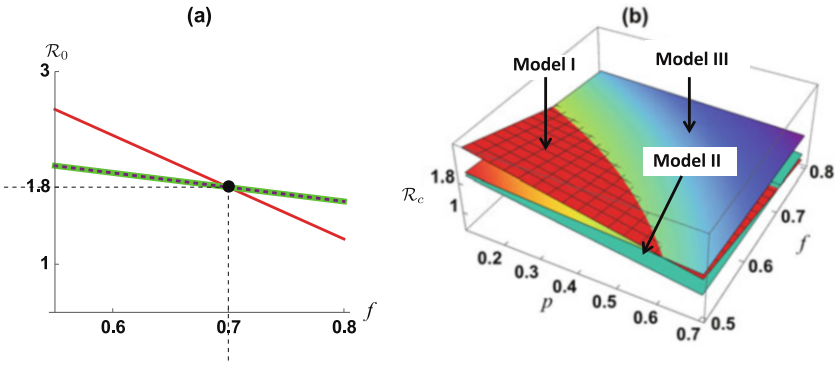

Fig. 10.13 Plots of the basic reproduction numbers (**a**) and control reproduction numbers (**b**) for the three models. In (**a**), $\mathscr{R}_0$ is plotted as a function of f for model I (thin solid), model II (dashed), and model III (thick solid). The parameter values are chosen such that all three $\mathscr{R}_{0i}$ have the same value 1.8 at $f = 0.7$ (note that $p = 0$). In (**b**), $\mathscr{R}_{Ci}$ is plotted as a function of p and f for models I—III. Other parameter values are given in the text

the three ODE models (10.20), (10.30), and (10.36), respectively. In the absence of hospitalization (i.e., $p = 0$), these $\mathscr{R}_{Ci}$ reduce to the corresponding basic reproduction numbers $\mathscr{R}_{0i}$ ($i = 1, 2, 3$). Figure 10.13 illustrates the difference between the basic and control reproduction numbers of the three models for a given set of parameter values, mostly based on the Ebola outbreak in West Africa in 2014. We fix all parameters except β_i ($i = I, H, D$) and f. Then, for a fixed value of $f_0 = 0.7$, we estimate β_i ($i = I, H, D$) from a given value of $\mathscr{R}_0$ (assumed to be the same for all three models). If we further assume that $\beta_H = \beta_D = 0.3\beta_I$, then we can get a unique value for β_I for fixed $\mathscr{R}_0$. Once we have the value of β_i, we have three functions of f, $\mathscr{R}_{0i}(f)$ ($i = 1, 2, 3$). For Fig. 10.13a, we used the common value of $\mathscr{R}_0(f_0) = 1.8$. The three curves are for model I (the thin solid curve), model II (the dashed curve), and model III (the think curve). For the selected set of parameter values, the $\mathscr{R}_0$ curves for models II and III overlap. The decreasing property of these curves represents the fact that higher disease mortality decreases $\mathscr{R}_{0i}(f)$, which is expected because the assumption that $\beta_D < \beta_I$. An interesting observation is that the dependence of the basic reproduction number on disease death f is more dramatic in model I than models II and III, particularly for smaller f values. For smaller values of f, model I tends to generate the highest $\mathscr{R}_0$, while for larger f values, model III provides higher $\mathscr{R}_0$. Other parameter values used are (time in days): $1/\gamma_{IR} = 18$, $1/\gamma_f = 2$, $1/\alpha = 9$. Parameters such as μ, χ_i ($i = 1, 2$) are calculated based on their relationships with the common parameters. For model III, additional parameter values include $1/\gamma_{IH} = 7$, $1/\gamma_{ID} = 8$, which can be used to determine γ_3 and ω_3 from (10.37).

When control is considered ($p > 0$), the dependence of $\mathscr{R}_{Ci}$ on p and f is illustrated in Fig. 10.13b. We observe that, for the given set of parameter values, model I (the darker surface with mesh) generates higher $\mathscr{R}_C$ values than models

II (the lighter surface) and III (the darker surface with no mesh) for smaller p and f, while model III provides the higher values for larger values of p and/or f. The differences in $\mathscr{R}_0$ and $\mathscr{R}_C$ between the three models indicate that model predictions about and evaluations of the effectiveness of control measures could be very different as well. Figure 10.14 shows numerical simulation results of the three ODE models (10.20), (10.30), and (10.36), which are reduced from the models I, II, and III, and presented in columns 1, 2, and 3, respectively. The A, B, and C panels correspond to three sets of (p, f) values: $(p, f) = (0, 0.7)$ (top panel), $(p, f) = (0.3, 0.5)$ (middle panel), and $(p, f) = (0.4, 0.7)$ (bottom panel). The top panel (A1–A3) is for the case of no hospitalization ($p = 0$). We observe that models II and III generate similar epidemic curves (fractions of infected individuals $(E + I + H)/N$), including peak sizes, times to peak, duration of epidemic (which lead to similar epidemic final sizes). Model I shows a higher peak size and an earlier time to peak. The middle panel (B1–B3) is for the case when the hospitalization is $p = 0.3$, and we observe that model I has the highest peak size while model II has the lowest. This is in agreement with the relative magnitudes of the control

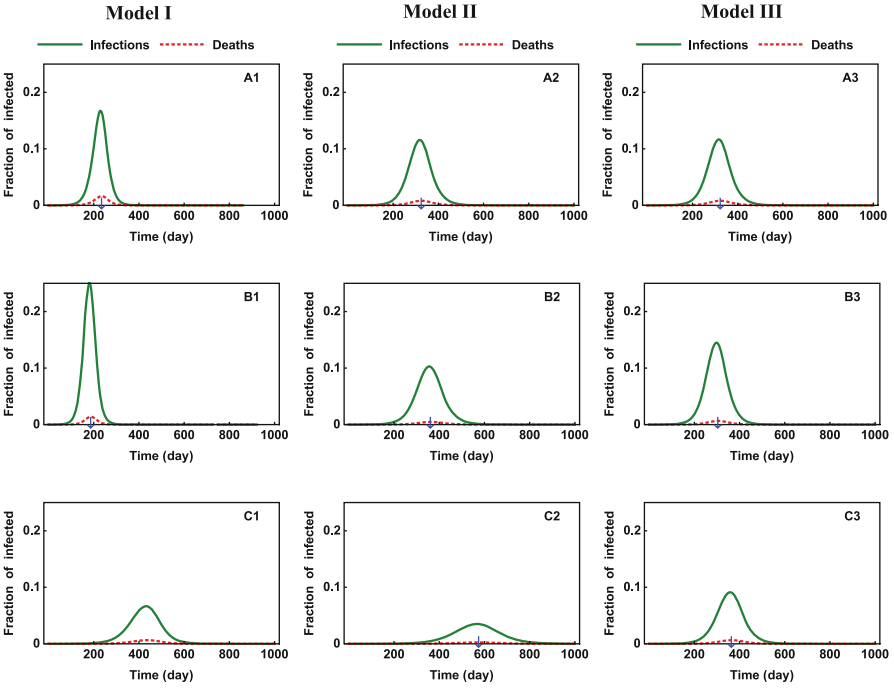

Fig. 10.14 Numerical simulations of the three ODE models (10.20), (10.30), and (10.36), which are reduced from the models I, II, and III, respectively. The fractions of infected individuals $(E + I + H)/N$ and death (D/N) are plotted over a time period of 1000 days. Three sets of (p, f) values are used: $(p, f) = (0, 0.7)$ (top row), $(p, f) = (0.3, 0.5)$ (middle row), and $(p, f) = (0.4, 0.7)$ (bottom row). Parameter values are the same as in Fig. 10.13

reproduction numbers $\mathscr{R}_{Ci}$, as the point $(p, f) = (0.3, 0.5)$ lies in the region where $\mathscr{R}_{C1} > \mathscr{R}_{C3} > \mathscr{R}_{C2}$ (see Fig. 10.13). For the bottom panel (C1–C3), because the point $(p, f) = (0.4, 0.7)$ lies in the region where $\mathscr{R}_{C3} > \mathscr{R}_{C1} > \mathscr{R}_{C2}$, we observe that model III generates the highest peak size while model II again has the lowest.

10.5 Slower than Exponential Growth

It has been standard practice in analyzing disease outbreaks to formulate a dynamical system as a deterministic compartmental model, then to use observed early outbreak data to fit parameters to the model, and finally to analyze the dynamical system to predict the course of the disease outbreak and to compare the effects of different management strategies. In general, such models predict an initial stochastic stage (while the number of infectious individuals is small), followed by a period of exponential growth. Measurement of this early exponential growth rate is an essential step in estimating contact rate parameters for the model. A thorough description of the analysis of compartmental models may be found in [21].

However, instances have been noted where the growth rate of an epidemic is clearly slower or faster than exponential. For example, [13], the 2013–2015 epidemic in West Africa has been viewed as a composition of locally asynchronous outbreaks at local levels displaying sub-exponential growth patterns during several generations. Specifically, if $I(t)$ is the number of infectious individuals at time t, a graph of $\log I(t)$ against t is a straight line if the growth rate is exponential, and for some disease outbreaks this has not been true. One of the earliest examples [16] concerns the growth of HIV/AIDS in the USA, and a possible explanation might be the mixture of short-term and long-term contacts. This could be a factor in other diseases where there are repeated contacts in family groups and less frequent contacts outside the home.

During the 2013–2015 Ebola epidemic in West Africa, in the country of Liberia, which has a total population size of 4,300,000, there were 10,678 suspected, probable, and confirmed cases of disease as of September 3, 2015 [32]. An SIR model for the whole country would have predicted more than 1,500,000 cases. This discrepancy cannot be explained by the assumption of control measures. In order to make plausible predictions of the effects of large-scale epidemics, it is necessary to use a phenomenological model based on observations in the early stages of the epidemic rather than to try to fit a mechanistic model. Some phenomenological models that have been used to good effect have been the generalized Richards model, the "generalized growth model," and the IDEA model.

10.5.1 The Generalized Richards Model

Perhaps the first attempt to fit early epidemic data is the Richards model [34]. This is a modification of the logistic population growth model, described in [22]

$$I'(t) = rI\left[1 - \left(\frac{I}{K}\right)^a\right].$$

In this model, I represents the cumulative number of infected individuals at time t, K is the carrying capacity or total case number of the outbreak, r is the per-capita growth rate of the infected population, and a is an exponent of deviation from the standard logistic model. The basic premise of the model is that the incidence curve has a single turning point t_m. The analytic solution of the model is

$$I(t) = \frac{K}{\left[1 + e^{-r(t-t_m)}\right]^{1/a}}.$$

10.5.2 The Generalized Growth Model

It has been pointed out [12–15, 39] that a so-called general growth model of the form

$$C'(t) = rC(t)^p,$$

where $C(t)$ is the number of disease cases occurring up to time t, and $p, 0 \leq p \leq 1$, is a "deceleration of growth" parameter, has exponential solutions if $p = 1$ but solutions with polynomial growth if $0 < p < 1$. This is not and does not claim to be a mechanistic epidemic model, but it has proved to be remarkably successful for fitting epidemic growth and predicting the course of an epidemic. For example, it has provided much better estimates of epidemic final size than the exponential growth assumption for the Ebola epidemic of 2014. However, it assumes a sustained increase in the number of disease cases and cannot capture the later decline in the number of new infections. Such phenomenological models are particularly likely to be suitable in situations where it is difficult to construct a mechanistic approach because of multiple transmission routes, interactions of spatial influences, or other aspects of uncertainty.

10.5.3 The IDEA Model

Another direction that would be well worth further exploration would be contact rates decreasing in time because of individual behavioral changes in response to a disease outbreak. A contact rate which is a decreasing function of time can certainly lead to early epidemic growth slower than exponential. A step in this direction has been initiated in a discrete model [19] that has been applied to an Ebola model in [20].

The IDEA model [19, 20, 37] is a discrete model that assumes damping of recruitment of new infections because of spontaneous or planned behavioral changes. It is assumed that the time interval in the model is equal to the duration of infection, so that the number of infective individuals at each stage is equal to the number of new infections. The resulting model is

$$I_t = \left[\frac{\mathscr{R}_0}{(1+d)^t}\right]^t.$$

Here, d is a discount factor describing the recruitment damping.

A variety of epidemiological situations in which slower than exponential epidemic growth might be possible have been described. Ultimately, the challenge for epidemiological modeling would be to determine which of these situations allow slower than exponential growth by deriving and analyzing mechanistic models to describe each of these situations. This is an important new direction for epidemic modeling. Some suggestions include metapopulation models with spatial structure including cross-coupling and mobility, clustering in spatial structure, dynamic contacts, agent-based models with differences in infectivity and susceptibility of individuals, and reactive behavioral changes early in a disease outbreak. It may well turn out that slower than exponential growth may be ruled out in some cases but is possible in others. For example, heterogeneity of mixing in a single location can be modeled by an autonomous dynamical system and the linearization theory of dynamical systems at an equilibrium shows that early epidemic growth for such a system is always exponential. On the other hand, metapopulation models may well allow many varieties of behaviors.

An important broader question is the matter of what information influences the behavior of people during a disease outbreak, and how to include this in a model. A recent book [28] describes some studies in this direction.

10.5.4 Models with Decreasing Contact Rates

There is anecdotal evidence that in an outbreak of a disease considered very serious there is early action to decrease the risk of being infected by decreasing contact rates. This early action may begin even before government efforts to combat the disease.

Since Ebola is a very serious disease, with case fatality rates of 70% or more, it is reasonable to assume a decreasing contact rate. This has been suggested in [1, 2]. In [1], an SIR model is assumed with a contact rate that decreases exponentially in time, and observations are used to estimate the rate of decrease. In [6], such a model is used to estimate the final size of an Ebola epidemic over a country using early growth rate data and this yields early final size estimates that are much closer to the eventual outbreak data than estimates assuming a constant contact rate. For example, for the 2014-5 Ebola outbreak in Guinea, a country with a total population size of 10,589,000 the assumption of a constant contact rate corresponding to $\mathscr{R}_0 = 1.5$ led to an estimate of more than 9,000,000 cases over the whole country, while a decreasing contact rate assumption led to an estimate of about 27,000 disease cases. The actual number of Ebola cases in Guinea in this outbreak was fewer than 4,000. The models described here are for an entire country and are not intended to replace more detailed models needed for disease management describing the progress of the disease in individual villages.

10.6 Project: Slower than Exponential Growth

We have suggested in Sect. 10.5.4 that slower than exponential growth of the number of infectious individuals may be explained by assuming a time-dependent decrease in the contact rate. The question of what modeling assumptions can lead to slower than exponential growth is a complex one [13]. Another possible explanation might be a decrease in contact rate depending on the current state of the system. If the model system remains autonomous, growth will remain exponential so long as the contact rate is a differentiable function of I so that the theory of linearization at a disease-free equilibrium remains valid. However, if the rate of new infections is $a\frac{S}{N}f(I)$ with $f(I)$ not differentiable at $I = 0$, different behavior is possible.

Consider an SIR model in which the equation for I is

$$I' = \beta \frac{S}{N} I^{\alpha} - \gamma I,$$

with $0 < \alpha < 1$. Initially, so long as $S \approx N$, we approximate this equation by

$$I' = \beta I^{\alpha} - \gamma I. \tag{10.40}$$

Question 7 Show that the basic reproduction number is

$$\mathscr{R}_0 = \frac{\beta}{\gamma}.$$

Question 8 Make the change of dependent variable $u = \log I$ and derive the differential equation satisfied by u.

Exponential growth of I corresponds to linear growth of u. It is clear that if $\alpha = 1$, u does grow linearly.

Question 9 Determine whether the rate of growth of u is less than linear for $\alpha < 1$, either by explicit solution of the equation for u or by simulations with $\beta > \gamma$ (so that $\mathscr{R}_0 > 1$) and a range of values of α.

10.7 Project: Movement Restrictions as a Control Strategy

Cordons Sanitaire or "sanitary barriers" are designed to prevent the movement, in and out, of people and goods from particular areas. The effectiveness of the use of *cordons sanitaire* has been controversial. This policy was last implemented nearly 100 years ago [9]. In desperate attempts to control disease, Ebola-stricken countries enforced public health officials decided to use this medieval control strategy in the EVD hot-zone, that is, the region of confluence of Guinea, Liberia, and Sierra Leone [30]. In this project, a framework that allows, in the simplest possible setting, the possibility of assessing the potential impact of the use of a *Cordon Sanitaire* during a disease outbreak is introduced. We consider an SIR epidemic model in two patches, one of which has a significantly larger contact rate, with short-term travel between the two patches. The total population resident in each patch is constant. We follow a Lagrangian perspective, that is, we keep track of each individual's place of residence at all times [4, 17]. This is in contrast to an Eulerian perspective, which describes migration between patches.

Thus we consider two patches, with total resident population sizes N_1 and N_2, respectively, each population being divided into susceptibles, infectives, and removed members. S_i and I_i denote the number of susceptibles and infectives, respectively, who are residents in Patch i, regardless of the patch in which they are present.

Residents of Patch i spend a fraction p_{ij} of their time in Patch j, with

$$p_{11} + p_{12} = 1, \quad p_{21} + p_{22} = 1.$$

The contact rate in Patch i is β_i, and we assume $\beta_1 > \beta_2$.

Each of the $p_{11}S_1$ susceptibles from Group 1 present in Patch 1 can be infected by infectives from Group 1 and from Group 2 present in Patch 1. Similarly, each of the $p_{12}S_1$ susceptibles present in Patch 2 can be infected by infectives from Group 1 and from Group 2 present in Patch 2.

Question 1 Show that the model equations are

$$S_i' = -p_{i1}S_i\left[p_{11}\frac{I_1}{N_1} + p_{12}\frac{I_2}{N_2}\right] - p_{i2}S_i\left[p_{21}\frac{I_1}{N_1} + p_{22}\frac{I_2}{N_2}\right]$$
$$I_i' = p_{i1}S_i\left[p_{11}\frac{I_1}{N_1} + p_{21}\frac{I_2}{N_2}\right] + p_{i2}S_i\left[p_{21}\frac{I_1}{N_1} + p_{22}\frac{I_2}{N_2}\right] - \gamma I_i, \quad i = 1, 2.$$

Question 2 Use the next generation matrix [38] to calculate the basic reproduction number.

Question 3 Use the approach described in Chaps. 4 and 5 to determine the final size relations.

Imposition of a *Cordon Sanitaire* amounts to replacing the fractions of normal travel between groups by

$$p_{11} = p_{22} = 1, \quad p_{12} = p_{21} = 0.$$

Question 4 Compare the reproduction numbers and final sizes with and without a *Cordon Sanitaire*, using numerical simulations with various parameter value choices.

The approach suggested here can be used with more detailed models for a specific disease, such as Ebola, in which transmission from one village to another through temporary visits is a factor [17].

10.8 Project: Effect of Early Detection

The following model for Ebola is considered in [10]:

$$\begin{aligned}
\frac{dS}{dt} &= -\beta S\frac{I + lJ}{N},\\
\frac{dE_1}{dt} &= \beta S\frac{I + lJ}{N} - k_1E_1,\\
\frac{dE_2}{dt} &= k_1E_1 - k_2E_2 - f_TE_2,\\
\frac{dI}{dt} &= k_2E_2 - (\alpha + \gamma)I,\\
\frac{dJ}{dt} &= \alpha I + f_TE_2 - \gamma_rJ,\\
\frac{dR}{dt} &= \gamma(1-\delta)I + \gamma_r(1-\delta)J,\\
\frac{dD}{dt} &= \gamma\delta I + \gamma_r\delta J,
\end{aligned} \tag{10.41}$$

where $N = S + E_1 + E_2 + I + J + R$. The variables E_1 and E_2 denote the numbers of latent undetectable and detectable individuals, respectively, I is the number of infectious individuals, J is the number of isolated infective individuals, R and D are numbers of recovered and dead due to the disease. For the parameters, β is the transmission rate, l is the relative transmissibility of isolated individuals, k is the rate of entering the detectable class, k_2 is the rate of becoming infective, f_T is the rate of being diagnosed, α is the rate of isolation, γ is the recovery rate, and γ_r is the rate at which individuals are removed from isolation after recovery or disease death.

References

1. Althaus, C.L. (2014) Estimating the reproduction number of Ebola Virus (EBOV) during the 2014 outbreak in West Africa, PLoS Currents: Edition 1. https://doi.org/10.1371/current.outbreaks.91afb5e0f279e7f29e7056095255b288.
2. Barbarossa, M.V., A Denes, G. Kiss, Y. Nakata, G. Rost, & Z. Vizi (2015) Transmission dynamics and final epidemic size of Ebola virus disease dynamics with varying interventions, PLoS One 10(7): e0131398. https://doi.org/10.1371/journalpone.0131398.
3. Bellan, S.E., J.R.C. Pulliam, J. Dushoff, and L.A. Meyers (2014) Ebola control: effect of asymptomatic infection and acquired immunity, The Lancet **384**:1499–1500.
4. Bichara, D., Y. Kang, C. Castillo-Chavez, R. Horan and C. Perringa (2015) SIS and SIR epidemic models under virtual dispersal, Bull. Math. Biol. **77**: 2004–2034.
5. Blower, S.M. and H. Dowlatabadi (1994) Sensitivity and uncertainty analysis of complex models of disease transmission: an HIV model, as an example. Int Stat Rev. **2**: 229–243.
6. Brauer, F. (2019) The final size of a serious epidemic, Bull. Math. Biol. https://doi.org/10.1017/s11538-018-00549-x
7. Browne, C.J., H. Gulbudak, and G. Webb (2015) Modeling contact tracing in outbreaks with application to Ebola, J. Theor. Biol. **384**: 33–49.
8. Butler, D. (2014) Models overestimate Ebola cases, Nature **515**: 18. https://doi.org/10.1038/515018a.
9. Byrne, J.P. (2008) Encyclopedia of Pestilence, Pandemics, and Plagues, **1** ABC-CLIO, 2008.
10. Chowell, D., C. Castillo-Chavez, S. Krishna, X. Qiu, and K.S. Anderson (2015) Modelling the effect of early detection of Ebola, Lancet Infectious Diseases, February, DOI: http://dx.doi.org/10.1016/S1473-3099(14)71084-9.
11. Chowell, G., N.W. Hengartnerb, C. Castillo-Chavez, P.W, Fenimore, and J.M. Hyman (2004) The basic reproductive number of Ebola and the effects of public health measures: the cases of Congo and Uganda, J. Theor. Biol. **229**: 119–126.
12. Chowell, G. and J. M. Hyman (2016) Mathematical and Statistical Modeling for Emerging and Re-emerging Infectious Diseases. Springer, 2016.
13. Chowell G., C. Viboud, J.M. Hyman, L. Simonsen (2015) The Western Africa Ebola virus disease epidemic exhibits both global exponential and local polynomial growth rates. PLOS Current Outbreaks, January 21.
14. Chowell, G. and C. Viboud (2016) Is it growing exponentially fast?–impact of assuming exponential growth for characterizing and forecasting epidemics with initial near-exponential growth dynamics Infectious Dis. Modelling **1**: 71–78.
15. Chowell, G., C. Viboud, L. Simonsen, & S. Moghadas (2016) Characterizing the reproduction number of epidemics with early sub-exponential growth dynamics, J. Roy. Soc. Interface: https://doi.org/10.1098/rsif.2016.0659.

16. Colgate, S.A., E. A. Stanley, J. M. Hyman, S. P. Layne, and C. Qualls (1989) Risk behavior-based model of the cubic growth of acquired immunodeficiency syndrome in the United States. Proc. Nat. Acad. Sci., textbf86: 4793–4797
17. Espinoza, B., V. Moreno, D, Bichara, and C. Castillo-Chavez (2016) Assessing the efficiency of movement restriction as a control strategy of Ebola, In Mathematical and Statistical Modeling for Emerging and Re-emerging Infectious Diseases, Springer International Publishing: pp. 123–145.
18. Feng, Z., Z. Zheng, N. Hernandez-Ceron, J.W. Glasser, and A.N. Hill (2016) Mathematical models of Ebola - Consequences of underlying assumptions, Math. Biosc. **277**: 89–107.
19. Fisman, D.N., T.S. Hauck, A.R. Tuite, & A.L. Greer (2013) An IDEA for short term outbreak projection: nearcasting using the basic reproduction number, PLOS One **8**: 1–8.
20. Fisman, D.N., E. Khoo, & A.R. Tuite (2014) Early epidemic dynamics of the west Africa 2014 Ebola outbreak: Estimates derived with a simple two-parameter model, PLOS currents **6**: September 8.
21. Hethcote, H.W. (2000) The mathematics of infectious diseases, SIAM Review **42**: 599–653.
22. Hsieh, Y.-H. (2009) Richards model: a simple procedure for real-time prediction of outbreak severity In Modeling and Dynamics of Infectious Diseases, pages 216–236. World Scientific.
23. Khan, A., M. Naveed, M. Dur-e-Ahmad, and M. Imran (2015) Estimating the basic reproductive ratio for the Ebola outbreak in Liberia and Sierra Leone, Infect. Dis. Poverty **4**.
24. Khan, A.S, F.K. Tshioko, D.L. Heymann, et al (1999) The reemergence of Ebola hemorrhagic fever, Democratic Republic of the Congo, 1995, J. Inf. Dis. **179**: S76–86.
25. King, K., et al (2015) Avoidable errors in the modelling of outbreaks of emerging pathogens, with special reference to Ebola, Proc. R. Soc. B **282**: 20150347. http://dx.doi.org/10.1098/rspb.2015.0347
26. Legrand, J., R.F. Grais, P.Y. Boelle, A.J. Valleron, and A. Flahault (2007) Understanding the dynamics of Ebola epidemics, Epidemiol. Infect **135**: 610–621.
27. Lewnard, J.A., M.L.N. Mbah, J.A. Alfaro-Murillo, et al. (2014) Dynamics and control of Ebola virus transmission in Montserrado, Liberia: a mathematical modelling analysis, Lancet Infect. Dis. **14**: 1189–1195.
28. Manfredi, P. & A. d'Onofrio (eds.) (2013) Modeling the Interplay between Human Behavior and the Spread of Infectious Diseases, Springer - Verlag, New York-Heidelberg-Dordrecht-London.
29. Meltzer M.I., C.Y. Atkins, S. Santibanez, et al. (2014) Estimating the future number of cases in the Ebola epidemic: Liberia and Sierra Leone, 2014–2015. MMWR Surveill. Summ. **63**: 2014–2015.
30. McNeil Jr., D.G. Jr. 9@014) NYT: Using a Tactic Unseen in a Century, Countries Cordon Off Ebola-Racked Areas, August 12, 2014.
31. Nishiura, H and G. Chowell (2014) Early transmission dynamics of Ebola virus disease (EVD), west Africa, March to August 2014, Euro Surveill. **19**: 1–6.
32. Nyenswah, T.G., F. Kateh, L. Bawo, M. Massaquoi, M. Gbanyan, M. Fallah, T. K. Nagbe, K. K. Karsor, C. S. Wesseh, S. Sieh, et al. (2016) Ebola and its control in Liberia, 2014–2015, Emerging Infectious Diseases **22**: 169.
33. Renshaw, E. (1991) Modelling Biological Populations in Space and Time. Cambridge University Press, Cambridge, 1991.
34. Richards, F. (1959) A flexible growth function for empirical use, J. Experimental Botany **10**: 290–301.
35. Rivers, C.M. et al. (2014) Modeling the impact of interventions on an epidemic of Ebola in Sierra Leone and Liberia, PLoS Current Outbreaks, November 6, 2014.
36. Towers, S., O. Patterson-Lomba, and C. Castillo-Chavez (2014) Temporal variations in the effective reproduction number of the 2014 West Africa Ebola Outbreak, PLoS Currents: Outbreaks **1**.
37. Tuite, A.R. & D.N. Fisman (2016) The IDEA model: A single equation approach to the Ebola forecasting challenge, Epidemics, http://dx.doi.org/10.1016/j.epidem.2016.09.001

38. van den Driessche, P. & J. Watmough (2002) Reproduction numbers and sub-threshold endemic equilibria for compartmental models of disease transmission. Math. Biosc., **180**: 29–48.
39. Viboud, C., L. Simonsen, and G. Chowell (2016) A generalized-growth model to characterize the early ascending phase of infectious disease outbreaks, Epidemics **15**: 27–37.
40. Webb G., C. Browne, X. Huo, O. Seydi, M. Seydi, and P. Magal (2014) A model of the 2014 Ebola epidemic in west Africa with contact tracing. PLoS Currents, https://doi.org/10.1371/currents.outbreaks.846b2a31ef37018b7d1126a9c8adf22a.
41. World Health Organization (WHO) (2001) Outbreak of Ebola hemorrhagic fever, Uganda, August 2000 - January 2001. Weekly epidemiological record 2001;76:41–48.